Mar Biol (2012) 159:2455–2478
DOI 10.1007/s00227-012-1904-y

ORIGINAL PAPER

Climate change effects on phytoplankton depend on cell size and food web structure

Toni Klauschies · Barbara Bauer · Nicole Aberle-Malzahn · Ulrich Sommer · Ursula Gaedke

Received: 18 October 2011 / Accepted: 17 February 2012 / Published online: 29 March 2012

Abstract We investigated the effects of warming on a natural phytoplankton community from the Baltic Sea, based on six mesocosm experiments conducted 2005–2009. We focused on differences in the dynamics of three phytoplankton size groups which are grazed to a variable extent by different zooplankton groups. While small-sized algae were mostly grazer-controlled, light and nutrient availability largely determined the growth of medium- and large-sized algae. Thus, the latter groups dominated at increased light levels. Warming increased mesozooplankton grazing on medium-sized algae, reducing their biomass. The biomass of small-sized algae was not affected by temperature, probably due to an interplay between indirect effects spreading through the food web. Thus, under the higher temperature and lower light levels anticipated for the next decades in the southern Baltic Sea, a higher share of smaller phytoplankton is expected. We conclude that considering the size structure of the phytoplankton community strongly improves the reliability of projections of climate change effects.

Communicated by R. Adrian.

T. Klauschies (✉) · B. Bauer · U. Gaedke
Institute of Biochemistry and Biology, University of Potsdam, Am Neuen Palais 10, 14469 Potsdam, Germany
e-mail: tklausch@uni-potsdam.de

B. Bauer
e-mail: barbara.bauer@uni-potsdam.de

U. Gaedke
e-mail: gaedke@uni-potsdam.de

B. Bauer · U. Sommer
Helmholtz Centre for Ocean Research Kiel (GEOMAR), Düsternbrooker Weg 20, 24105 Kiel, Germany

U. Sommer
e-mail: usommer@ifm-geomar.de

N. Aberle-Malzahn
Alfred Wegener Institute for Polar and Marine Research at Biologische Anstalt Helgoland, Kurpromenade C-47, 27498 Helgoland, Germany
e-mail: Nicole.Aberle-Malzahn@awi.de

Introduction

Marine phytoplankton contribute to the biological regulation of the climate and provide half of the world's primary production (Baumert and Petzoldt 2008; Boyce et al. 2010). As primary producers, phytoplankton supplied the energy basis of pelagic and benthic food webs, and potential changes in the structure and dynamics of marine phytoplankton communities under climate change are a reason for concern. According to the IPCC report (2007), regions in the higher latitudes of the Northern Hemisphere are expected to experience the most pronounced changes during the next 100 years, including earlier warming in the spring, which is the most decisive season in the yearly phytoplankton development. It is therefore particularly relevant to study the response of phytoplankton communities to increased temperature during the spring, to estimate effects of future climate change on aquatic food webs.

Boyce et al. (2010) proposed that increasing sea surface temperatures resulted in the recent global decrease in phytoplankton biomass. However, the observed patterns strongly differed at the regional scale, for example in the western Baltic Sea. Phytoplankton biomass decreased by 50 % since 1979 in the Kattegat (Henriksen 2009), whereas it increased by a factor of two in the Kiel Fjord over the past 100 years (Wasmund et al. 2008). This example points to the need to better understand the processes that regulate

phytoplankton dynamics both for analysing current trends and for making projections into the future.

Climate change is not restricted to temperature change, but cloudiness and hence surface irradiance are predicted to change as well. This holds also for the Baltic Sea area, where latitude-dependent decreases and increases in cloudiness have already been observed (BACC 2008; Lehmann et al. 2011). The response of phytoplankton to irradiance is strong, and under natural conditions, light intensity varies more in early spring than temperature. Temperature and irradiance may have interacting effects on phytoplankton growth and mortality. Thus, to predict effects of warming on phytoplankton communities, different light intensities have to be considered.

The spring phytoplankton bloom is induced by favourable nutrient and light conditions and declines when mortality surpasses growth, either because growth becomes nutrient limited or because the mortality rate increases due to higher zooplankton grazing and/or sedimentation (Sommer 2005; Thackeray et al. 2008; Wiltshire et al. 2008). Temperature directly alters photosynthesis and respiration rates; however, the indirect effect of increased grazing may outweigh these direct effects (Gaedke et al. 2010). Thus, food web interactions need to be considered when assessing temperature effects on phytoplankton. A decisive trait influencing food web interactions within phytoplankton communities is size. Phytoplankton groups of different size are grazed by different groups of grazers and differ in their sensitivity to abiotic forces such as temperature, light and nutrients. Their reaction to climate change will also likely be different, which will affect both the phytoplankton community composition and the dynamics of the total community biomass.

Micro- and mesozooplankton are the major consumers of phytoplankton (Sommer 2005). Copepods preferentially feed upon phytoplankton and microzooplankton with particle sizes between 1,000 μm^3 (Sommer and Stibor 2002; Hansen et al. 1994) and 100,000 μm^3 (Hansen et al. 1994), whereas ciliates mainly consume prey items in the ESD range of 2–20 μm (<5,000 μm^3) (Montagnes 1996; Tadonleke and Sime-Ngado 2000; Johansson et al. 2004). Hence, these two zooplankton groups likely differ in their top-down control of differently sized phytoplankton and have to be considered separately.

We analysed mesocosm experiments to investigate the regulation and response of different size groups of phytoplankton to temperature under various light regimes and grazer abundances. These experiments were conducted in 2005–2009 in Kiel with natural spring-time plankton communities from the Baltic Sea. Our study focused on three phytoplankton size categories: small (particle size <1,500 μm^3), medium (1,500–45,000 μm^3) and large (>45,000 μm^3) algae, which differ in their edibility for the various grazers (Fig. 1) and compete for nutrients and light.

Small-sized algae are mainly eaten by ciliates, which, in comparison with copepods and heterotrophic dinoflagellates, respond faster to altered food conditions given their higher mass specific ingestion and growth rates (Ingrid et al. 1996; Hansen et al. 1997; Löder et al. 2011a, b). Therefore, we hypothesize that small-sized algae are more controlled by their grazers than medium-sized algae, which are mainly consumed by copepods and heterotrophic dinoflagellates. However, increasing temperature might alter the importance of grazing for the different groups as an increase in temperature strengthens predator–prey interactions (Barton et al. 2009; O'Connor 2009; Beveridge et al. 2010a, b; Hoekman 2010). Thus, grazing pressure on medium-sized algae might increase with increasing temperature. Microzooplankton grazers of small-sized algae are themselves controlled by mesozooplankton (Calbet and Saiz 2005; Sommer et al. 2005a, b; Sherr and Sherr 2007, 2009; Saiz and Calbet 2011). The growth of these two grazer groups are similarly accelerated by increasing temperatures (Rose and Caron 2007). Therefore, the effect of an increase in the grazing rates of microzooplankton at higher temperature may be counteracted by a decrease in their biomass due to more active mesozooplankton. In addition, decreased biomass of medium-sized algae due to mesozooplankton grazing will release both small- and large-sized algae from competition with medium-sized algae for nutrients. Large-sized algae are, due to their size or defence structures, mostly inedible for micro- and mesozooplankton, except for some large thecate heterotrophic

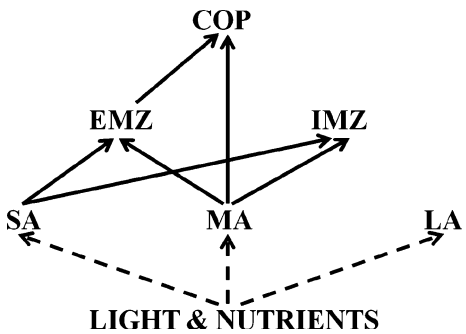

Fig. 1 Sketch of the food web in our study system, comprising the most important groups of phytoplankton and zooplankton. COP stands for copepods, EMZ and IMZ for microzooplankton (ciliates and heterotrophic dinoflagellates), which are edible (EMZ) or inedible (IMZ) for copepods, SA for small-sized algae containing pico- and single-cell nanophytoplankton <1,500 μm^3, MA for medium-sized algae containing micro- and chain-forming nanophytoplankton in the particle size range of 1,500–45,000 μm^3 and LA for large-sized algae containing microphytoplankton >45,000 μm^3 or armoured forms. *Solid arrows* indicate predation. *Dashed arrows* indicate autotrophic resource use. *Arrow* direction was chosen according to energy flow

dinoflagellates (Sherr and Sherr 2009; Löder et al. 2011b). Hence, we expect that large-sized algae are primarily regulated by nutrient availability. Thus, we tested the following hypotheses

H1 The three algal size groups differ in the regulation of their spring development under ambient-temperature conditions.

H1(1) Small-sized algae are mainly regulated by their grazers.

H1(2) Medium- and large-sized algae are mainly regulated by nutrient and light availability.

H2 Increasing temperature alters the relative importance of light, nutrients and grazing intensity in regulating the phytoplankton bloom.

H2(1) Grazing on small-sized algae is little affected due to indirect food web effects.

H2(2) Warming enhances the grazing pressure on medium-sized algae due to increased grazing activity of heterotrophic dinoflagellates and copepods.

H2(3) The bottom-up control of large-sized algae declines due to reduced competition with medium-sized algae.

H2(4) The share of small-sized algae in the phytoplankton community increases.

Methods

Mesocosm experiments

Experimental design

The experimental set-up consisted of 8 (2005–2007) or 12 (2008–2009) mesocosms in temperature-controlled rooms. Mesocosms had a volume of 1,400 L and were filled with unfiltered seawater from the Kiel Fjord, containing overwintering populations of phytoplankton, microzooplankton and bacteria. Mesozooplankton (mainly copepods) were added from net catches, in different amounts among years. During the first 4 experiments (2005, 2006-1, 2006-2 and 2007), 4 temperature levels were applied within each experiment. In these years, light levels were the same within one experiment, but varied between experiments. The experiment in 2008 consisted of a factorial combination of two temperature levels and 3 light levels, and the experiment in 2009 had a factorial combination of two temperature levels and 3 initial mesozooplankton (copepod) abundance levels. In all experiments, the temperature regime was programmed according to the decadal mean (1993–2002) local sea surface temperatures and elevated by 0, 2, 4 and 6 °C for the different temperature treatments. Irradiance was calculated according to astronomic models (Brock 1981) and reduced to represent clouds and underwater light attenuation. We grouped the light treatments into two categories: low-light experiments with initial light intensities 1.03 (2005) and 2.06 (2007) Watt m^{-2} d^{-1} and high-light experiments with initial light intensities 4.12 (2006-2), 4.78 (2009), 4.88, 5.68, 6.17 (2008) and 6.43 (2006-1) Watt m^{-2} d^{-1}. Detailed descriptions of the experiments have been published previously (Sommer et al. 2007; Sommer and Lengfellner 2008; Lewandowska and Sommer 2010; Sommer and Lewandowska 2011).

During the experiments, the natural seasonal temperature and light increase were simulated. Seasonal light and temperature programmes were set to start on 4th of February in the experiments 2005–2007 and 15th of February in the experiments 2008 and 2009. Experiments lasted for 5½ to 12 weeks.

Sampling

Phytoplankton samples were taken 3 times per week and zooplankton samples once per week. Phytoplankton >5 µm and microzooplankton were counted using a microscope, and cell volumes were estimated after microscopic measurements (Hillebrand et al. 1999) and converted to biomass according to Menden-Deuer and Lessard (2000) and Putt and Stoecker (1989). Abundance and biomass of phytoplankton <5 µm were measured by flow cytometry. Primary production was measured according to the ^{14}C incubation method (Gargas 1975).

Phytoplankton

Phytoplankton was divided into three groups: small-sized algae (SA, particle size <1,500 μm^3), medium-sized algae (MA, 1,500–45,000 μm^3) and large-sized algae (LA, >45,000 μm^3 or defence structure against zooplankton grazing) (Appendix 1). The small-sized algae comprised autotrophic pico- and single-celled nanophytoplankton, that is diatoms, autotrophic athecate and thecate dinoflagellates, Haptophyceae, Chrysophyceae, and Cryptophyceae. The medium-sized algae comprised micro- and chain-forming nanophytoplankton, that is diatoms, silicoflagellates, Chryptophyceae, Chlorophyceae, and autotrophic athecate and thecate dinoflagellates. The large-sized algae are comprised of diatoms and autotrophic thecate dinoflagellates.

Microzooplankton

Microzooplankton was split into two groups: *edible microzooplankton* (EMZ) and *inedible microzooplankton* (IMZ) (Appendix 2). The first group was comprised of ciliates, athecate and thecate heterotrophic dinoflagellates,

which are preferred prey for copepods. The second group comprised species that are mostly inedible for copepods, that is large ciliates.

Mesozooplankton

Mesozooplankton comprised mainly calanoid and cyclopoid copepods, for example *Oithona similis*, *Pseudocalanus/Paracalanus* sp., *Centropages typicus*, *Temora longicornis* and *Acartia tonsa*.

Statistical analysis of the bottom-up factors nutrient and light

To estimate the role of nutrient depletion in the breakdown of the phytoplankton bloom, we compared the date of the local biomass maximum of the phytoplankton size groups during the bloom with the onset of a potential nutrient depletion (which will be referred to as 'onset of nutrient depletion' in the following) separately for the ambient ($\Delta T = 0$, $\Delta T = 2$ °C)- and warm ($\Delta T = 4$, $\Delta T = 6$ °C)-temperature treatments. We defined the onset of nutrient depletion as the day when nutrients dropped below specific threshold values. These values were the general half-saturation constants (k_N) of nutrient-limited phytoplankton growth (nutrient concentrations where the phytoplankton growth rate is half of the maximum). We used the threshold values 0.1 (phosphate), 5 (silicate) and 1 (nitrogen) μ mol L^{-1} for analyses. We related peak time with the date where nutrient concentrations dropped below the threshold level using linear regression. As the biomass of LA was too low in the experiments 2005 and 2007, no comparison was made between the peak time of LA and the date of the onset of its potential nutrient limitation for these years. The experiment 2006-1 was not considered because nutrient data were not available. Temperature-induced changes in the date of the onset of a potential nutrient depletion were investigated using a Wilcoxon's rank sum test. We used a sign test to assess whether the number of mesocosms where the onset of a potential nutrient limitation preceded the peak time was significant compared to the total number of mesocosms considered.

To assess the influence of light on the biomass development of the phytoplankton groups, we related the initial light intensity of the experiments to the local maximum biomass of the phytoplankton size groups during the bloom and to their mean net growth rates (measured before their biomass peaks) using linear and non-linear regressions. The mean net growth rate was calculated according to the formula:

$$R = \sqrt[t]{\frac{B_{\text{peak time}}}{B_0}},$$

where $B_{\text{peak time}}$ is the local maximum biomass during the bloom, B_0 the initial biomass and t the period until the biomass peak was reached. Decline of the primary production to biomass ratio (P/B) of the whole phytoplankton community after the bloom indicated that the breakdown of the bloom was caused by bottom-up factors. Therefore, we considered the time series of the P/B.

Statistical analysis of grazing and food web structure

To gain insights into the predator–prey relationships in the mesocosms, we studied the biomass dynamics of the phyto- and zooplankton groups. Additionally, we related the mean biomass of the various prey and predator groups separately for the high-light and low-light experiments and for the ambient- and warm-temperature treatments using linear regression. The high-light experiments 2006-1 and 2006-2 were excluded because they started already close to bloom conditions and thus biotic interactions did not play a major role. Moreover, microzooplankton data are not available for the experiment 2006-1. With spring phytoplankton blooms, constantly increasing light levels promote the development of a high biomass before nutrient limitation or self-shading becomes important. However, in the case of strong top-down control, grazers suppress algal biomass growth. Thus, we assumed that in our system, mainly top-down-controlled prey populations show a lower temporal variability of biomass than bottom-up-controlled ones. Thus, we calculated the coefficient of variation (CV, standard deviation divided by mean) of the time series of the biomass of the different phytoplankton groups to estimate the strength of their top-down control and related it to initial light intensities using linear regressions, applied separately for the ambient- and warm-temperature treatments. The CV of the LA was not calculated for the low-light experiments 2005 and 2007 as their biomass was mainly around the detection level.

A further indication that the breakdown of the phytoplankton bloom is caused primarily by increased grazing is when a substantial part of the primary production of the phytoplankton groups is consumed by their predators and converted into predator biomass. Thus, we calculated a grazing pressure index (GPI) for small- and medium-sized algae at their particular peak time, respectively, according to the formula:

$$\text{GPI}_{\text{SA}} = \frac{\text{EMZ} + \text{IMZ}}{\text{PP} \cdot \frac{\text{SA}}{\text{PC}}}$$

$$\text{GPI}_{\text{MA}} = \frac{\text{COP} + \text{NAUP}}{\text{PP} \cdot \frac{\text{MA}}{\text{PC}}},$$

where SA, MA, EMZ, IMZ, COP and NAUP are the biomasses of the different phyto- and zooplankton groups we considered (Fig. 1), and PC and PP the biomass and the measured primary production of the total phytoplankton community. The grazing pressure indices were related to

initial light intensities separately for the ambient- and warm-temperature treatments using linear regression.

A Wilcoxon's rank sum test was used to compare averaged parameters of the different phytoplankton size groups. To preclude compensatory effects within the EMZ between different groups of organisms, we also considered the response of smaller and larger ciliates and heterotrophic dinoflagellates.

Statistical analysis of the shifts in community composition

In order to investigate temperature- and light-induced shifts in the community composition, we calculated the temporal mean relative biomass and the relative biomass during the bloom of the three phytoplankton groups SA, MA and LA. We related these to initial light intensities by applying linear and non-linear regression separately for the ambient- and warm-temperature treatments. The timing of the phytoplankton bloom is defined as the date of the maximum biomass of the total phytoplankton community.

Statistical test of temperature effects

To establish statistically robust temperature effects, two test procedures were used. According to Juliano (2001), we tested for differences in the parameters of the linear and non-linear regression at different temperatures using an indicator variable. To compare linear and non-linear responses of dependent variables at two ($\Delta T = +0$ °C, +6 °C) or four ($\Delta T = +0$ °C, +2 °C, +4 °C, +6 °C) different temperatures, we used the implicit functions

$$Y = (A + j \cdot T_A) \cdot \left(\frac{X}{(B + j \cdot T_B) + X} \right) - 1 (\text{saturation}),$$

$$Y = (A + j \cdot T_A) \cdot \frac{1}{X} (\text{hyperbola}),$$

$$Y = (A + j \cdot T_A) \cdot X + (B + j \cdot T_B) (\text{linear}),$$

where j is an indicator variable that takes on the values 0, 1, 2 and 3 for temperature treatments $\Delta T = +0$ °C, +2 °C, +4 °C, +6 °C, respectively. The parameters T_A and T_B represent the differences between temperature treatments for parameters A and B, either two (if only the high-light experiments of 2008 and 2009 were considered) or four (if either the low-light or all experiments were considered) (Juliano 2001). If T_A and T_B are significantly different from zero, then the dependent variables differ significantly in their response at different temperatures (Juliano 2001). As a second method, the Wilcoxon's rank sum test was used, where we grouped data from the two lower-temperature treatments ($\Delta T = +0$ °C, +2 °C) and compared it to the grouped data from the two higher-temperature treatments ($\Delta T = +4$ °C, +6 °C), as in Figs. 6, and 7. We assumed significant temperature effects if both the Juliano's test and the Wilcoxon's rank sum test revealed a significance level of at least 0.05.

MATLAB 7.5 was used for preparing graphs and for statistical analysis.

Results

Bottom-up regulation by nutrients and light under ambient ($\Delta T = 0$ °C and $\Delta T = 2$ °C)-temperature conditions

The phytoplankton community showed a typical spring development in all experiments. Depending on the phytoplankton group and the abiotic forcing regime, the phytoplankton biomass grew exponentially with a time delay of up to 40 days for 1–3 weeks and declined after reaching its peak. The phytoplankton biomass increase was accompanied by a rapid decrease in nutrients. The concentrations of the different dissolved nutrients (P, N, Si) dropped below the threshold values, indicating nutrient depletion (see "Methods") almost simultaneously. The only exception was in the low-light experiments with respect to N.

Small-sized phytoplankton (SA)

To estimate the role of nutrient depletion for the timing and height of the biomass peak, we related the peak time to the date of the onset of a potential nutrient depletion. Nutrient concentrations often fell below the threshold level only after the biomass maximum of SA was reached, and the peak time of SA and the onset of nutrient depletion were neither in the low-light nor in the high-light experiments correlated (Table 1; Fig. 2a, d). These results indicate that nutrient depletion was not the major factor in the breakdown of the SA bloom. In addition, SA biomass increased again after the bloom in some of the low-light experiments (Fig. 4), which suggests that nutrient depletion was not severe for SA.

The influence of the other bottom-up regulation factor, light, on the growth of SA was also small compared to its effect on the growth of MA and LA (Fig. 3), although the biomass maximum and the mean net growth rate of SA were positively related to the initial light intensity (Table 2; Fig. 3a, d). In particular, the increase in the biomass of MA and LA with increasing light exceeded that of SA by more than an order of magnitude (Fig. 3).

Medium- (MA) and large-sized algae (LA)

Peak values of MA and LA were strongly regulated bottom-up by nutrients and light. In contrast to SA, the timing

Table 1 Results of linear regressions with the peak time of small- (SA), medium- (MA) and large-sized algae (LA) as dependent and the onset of nutrient depletion (potentially caused by silicate, phosphorus, or nitrogen) as independent variable, separately for ambient (ΔT=0 °C, ΔT=2 °C) and warm (ΔT=4 °C, ΔT=6 °C) temperature treatments (columns 1–9), and results of the sign test (column 10)

Group	Nutrient	Treatment	Linear regression					°C (Juliano's test)	Sign test	°C (Wilcoxon's rank sum test)	
			N	Slope	Intercept	R^2	*P* value	*P* value	*P* value	Mean ± SD	*P* value
			High-light								
SA	Silicate	Ambient	16	−0.09	14.68	0.01	n.s.	n.s.	n.s.	−1.06 ± 6.53	n.s.
		Warm	16	−0.55	16.67	0.52	<0.01		n.s.	0.25 ± 5.89	
	Phosphorus	Ambient	16	−0.23	16.18	0.05	n.s.	n.s.	n.s.	1.00 ± 6.20	n.s.
		Warm	16	−0.81	18.41	0.60	<0.001		n.s.	1.34 ± 5.06	
	Nitrogen	Ambient	16	−0.14	15.26	0.02	n.s.	n.s.	n.s.	−0.13 ± 6.38	n.s.
		Warm	16	−0.68	17.74	0.58	<0.001		n.s.	0.69 ± 5.44	
MA	Silicate	Ambient	16	0.83	4.35	0.89	<0.001	n.s.	<0.01	1.94 ± 1.57	n.s.
		Warm	16	0.82	3.32	0.92	<0.001		<0.001	1.44 ± 1.09	
	Phosphorus	Ambient	16	0.99	4.11	0.86	<0.001	n.s.	<0.001	4.00 ± 1.55	<0.01
		Warm	16	1.10	1.65	0.89	<0.001		<0.001	2.56 ± 1.03	
	Nitrogen	Ambient	16	0.88	4.52	0.84	<0.001	n.s.	<0.001	2.88 ± 1.71	<0.1
		Warm	16	0.93	2.58	0.86	<0.001		<0.001	1.88 ± 1.15	
LA	Silicate	Ambient	16	1.03	5.51	0.70	<0.001	n.s.	<0.001	6.00 ± 3.16	n.s.
		Warm	16	1.41	0.36	0.34	<0.05		<0.05	4.69 ± 7.10	
	Phosphorus	Ambient	16	1.25	5.02	0.69	<0.001	n.s.	<0.001	8.06 ± 3.34	n.s.
		Warm	16	1.78	−1.57	0.30	<0.05		<0.05	5.81 ± 7.46	
	Nitrogen	Ambient	16	1.08	5.80	0.66	<0.001	n.s.	<0.001	6.94 ± 3.40	n.s.
		Warm	16	1.47	0.36	0.27	<0.05		<0.05	5.13 ± 7.44	
			Low-light								
SA	Silicate	Ambient	8	0.57	22.52	0.22	n.s.	n.s.	n.s.	0.50 ± 5.42	n.s.
		Warm	8	0.65	15.79	0.59	<0.05		n.s.	−1.00 ± 3.38	
	Phosphorus	Ambient	8	0.40	32.94	0.31	n.s.	n.s.	n.s.	4.50 ± 6.70	<0.05
		Warm	8	0.53	21.04	0.48	<0.1		n.s.	−1.34 ± 4.17	
MA	Silicate	Ambient	8	0.75	11.92	0.43	<0.1	n.s.	n.s.	−1.13 ± 4.28	<0.1
		Warm	8	1.16	−4.60	0.69	<0.05		<0.1	2.75 ± 4.13	
	Phosphorus	Ambient	8	0.50	26.84	0.53	<0.05	n.s.	n.s.	2.88 ± 5.44	n.s.
		Warm	8	1.01	2.01	0.63	<0.05		n.s.	2.34 ± 4.44	

We used the latter to assess if the number of mesocosms where the onset of a potential nutrient limitation preceded the peak time was significant compared to the total number of mesocosms considered. Last two columns (11 and 12) give evidence if averaged differences between the peak time of the different phytoplankton size groups and the onset of a potential nutrient depletion (mean ± standard deviation) (column 11) are significantly different between ambient and warm temperature treatments

of the biomass maxima of MA and LA was positively related to the onset of nutrient depletion in the high-light experiments. Nutrient concentrations dropped below their threshold values before the biomass maxima of MA and LA were reached (on average 2.94 ± 1.79 and 7.00 ± 3.34 days, mean ± SD, $N = 48$, resp.; Table 1; Fig. 2b, c). In the low-light experiments, the peak time of MA and the onset of nutrient depletion were uncorrelated except for phosphorus (Table 1; Fig. 2e). The slower nutrient depletion at low light was most likely due to low net biomass production.

The biomass maximum of MA strongly increased with light up to a value of circa 3 Watt $m^{-2}d^{-1}$ (Table 2; Fig. 3b). The mean net growth rate of MA and the maximum biomass of LA also were considerably higher at high-light than at low-light conditions (Table 2; Fig. 3c, e), suggesting strong light limitation at low-light conditions. In addition, in high-light experiments, the mean net growth rates of MA and LA are 2.5 (Wilcoxon's rank sum test, $N_1 = 40$, $N_2 = 40$, $P < 0.001$) and 1.5 (Wilcoxon's rank sum test, $N_1 = 40$, $N_2 = 38$, $P < 0.01$) times higher than that of SA, respectively (Fig. 3d–f), indicating higher

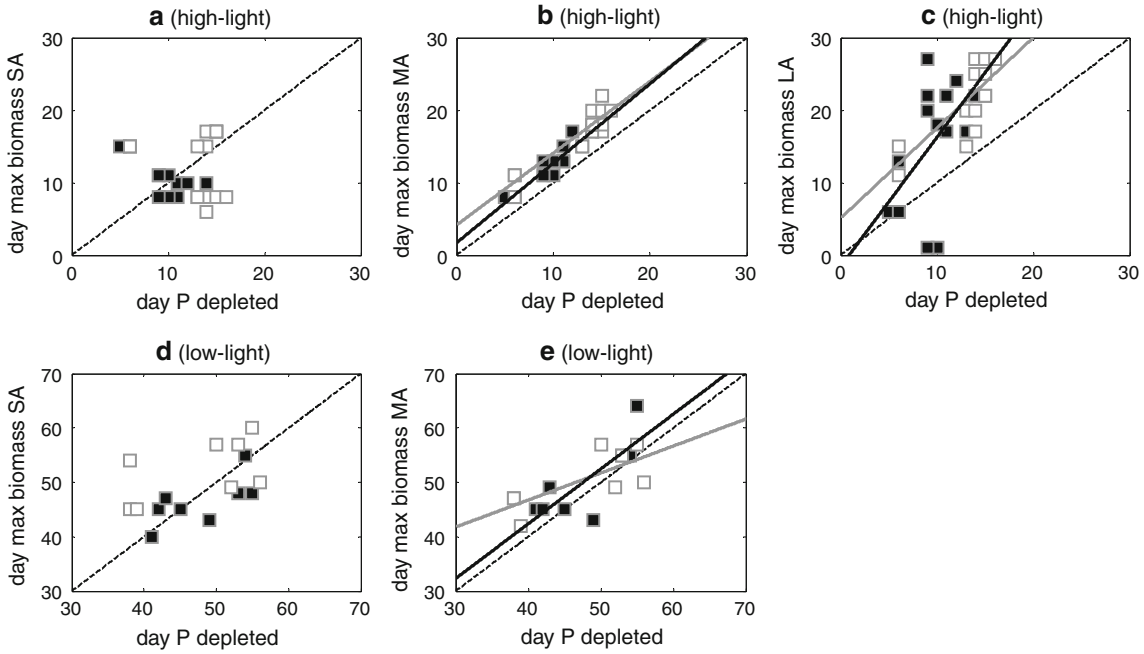

Fig. 2 The date of the maximum biomass of small- (SA, **a**, **d**), medium- (MA, **b**, **e**) and large-sized (LA, **c**) algae in the high-light (**a**–**c**) and low-light (**d**, **e**) experiments in relation to the date of the onset of potential phosphorus depletion. Latter is defined as the first day when dissolved phosphorus concentration dropped below the threshold value of 0.1 μ mol L^{-1}. The *dashed line* represents a one-to-one relationship. Data points above the *line* indicate that the nutrient depletion started before the biomass maximum of the respective algal size group was reached. Data points below the line indicate that the nutrients were not yet exhausted at the time of the biomass maximum of the respective algal size group. *White squares* indicate data from the ambient ($\Delta T = 0$ °C, $\Delta T = 2$ °C)- and *black squares* from the warm-temperature treatments ($\Delta T = 4$ °C, $\Delta T = 6$ °C). *Grey* ($\Delta T = 0$ °C, $\Delta T = 2$ °C) and *black* ($\Delta T = 4$ °C, $\Delta T = 6$ °C) *lines* represent significant ($P < 0.05$) linear regression *lines* with positive slopes. Similar patterns were observed for N and Si

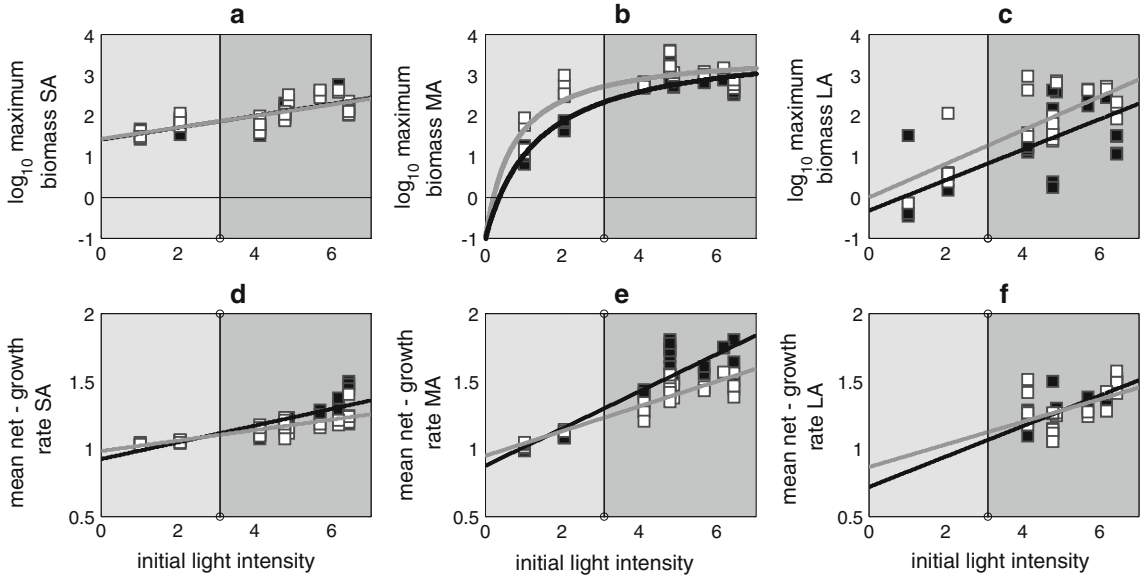

Fig. 3 Maximum biomasses [μg C L^{-1}] (**a**–**c**) and mean net growth rates [d^{-1}] of small- (SA, **a**, **d**), medium- (MA, **b**, **e**) and large-sized (LA, **c**, **f**) algae in relation to the initial light intensity [Watt m^{-2} d^{-1}] of the experiments. The mean net growth rate R is calculated according to the formula $R = (B_{\text{peak time}} \bullet B_0^{-1})^{1/t}$ where $B_{\text{peak time}}$ is the local maximum biomass during the bloom, B_0 the initial biomass and t the period until the biomass peak was reached. White squares indicate data from the ambient ($\Delta T = 0$ °C, $\Delta T = 2$ °C)- and black squares from the warm-temperature treatments ($\Delta T = 4$ °C, $\Delta T = 6$ °C). Low-light and high-light experiments are marked light and *dark grey*, respectively. *Grey* ($\Delta T = 0$ °C, $\Delta T = 2$ °C) and *black* ($\Delta T = 4$ °C, $\Delta T = 6$ °C) *curves* represented significant ($P < 0.05$) linear (**a**, **c**–**e**) and non-linear (**b**) regression *lines*. Latter correspond to the formula $y = y_{\max} \bullet (x \bullet (k + x)^{-1}) - 1$

Table 2 Results of linear and non-linear regressions relating different parameters of small- (SA), medium- (MA) and large-sized algae (LA), copepods (COP), nauplii (NAUP), edible (EMZ) and inedible microzooplankton (IMZ), smaller (CS) and larger ciliates (CL) and heterotrophic dinoflagellates (DINO) to initial light intensity for ambient ($\Delta T = 0$ °C, $\Delta T = 2$ °C)- and warm ($\Delta T = 4$ °C, $\Delta T = 6$ °C)-temperature treatments

Plankton group	Treatment	Linear regression					°C (Juliano's test)	°C (Wilcoxon's rank sum test)	
		N	Slope (*s*)	Intercept (*i*)	R^2	*P* value	*P* value	*P* value	
								Low-light	High-light
				Maximum biomass					
SA	Ambient	28	0.14	1.43	0.57	<0.001	n.s.	n.s.	n.s.
	Warm	28	0.15	1.42	0.54	<0.001			
LA	Ambient	28	0.45	−0.20	0.66	<0.001	n.s.	n.s.	<0.05
	Warm	28	0.35	−0.15	0.45	<0.001			
COP	Ambient	24	−0.05	1.78	0.06	n.s.	n.s.	n.s.	n.s.
	Warm	24	0.02	1.69	0.01	n.s.			
NAUP	Ambient	24	−0.04	0.98	0.04	n.s.	<0.01 (s)	n.s.	<0.001
	Warm	24	0.15	0.50	0.45	<0.001			
EMZ	Ambient	24	0.11	0.76	0.14	<0.1	n.s.	n.s.	n.s.
	Warm	24	0.20	0.43	0.29	<0.01			
IMZ	Ambient	18	−0.03	0.06	0.01	n.s.	n.s.	n.s.	n.s.
	Warm	20	−0.14	0.50	0.13	n.s.			
CS	Ambient	24	0.16	0.37	0.23	<0.05	n.s.	n.s.	n.s.
	Warm	24	0.23	0.14	0.52	<0.001			
CL	Ambient	24	−0.24	1.29	0.34	<0.01	n.s.	n.s.	n.s.
	Warm	23	−0.17	0.76	0.14	<0.1			
DINO	Ambient	20	0.26	−0.80	0.24	<0.05	n.s.	n.s.	n.s.
	Warm	20	0.34	−0.95	0.22	<0.05			
				Mean net growth rate					
SA	Ambient	28	0.04	0.98	0.70	<0.001	<0.01 (s) <0.1 (i)	n.s.	n.s.
	Warm	28	0.06	0.92	0.70	<0.001			
MA	Ambient	28	0.09	0.94	0.85	<0.001	<0.01 (s)	n.s.	<0.001
	Warm	28	0.14	0.87	0.81	<0.001			
LA	Ambient	20	0.08	0.86	0.24	<0.05	n.s.	n.s.	n.s.
	Warm	18	0.11	0.71	0.47	<0.01			
				Grazing pressure index (GPI)					
SA	Ambient	24	−0.02	−0.62	0.00	n.s.	n.s.	n.s.	n.s.
	Warm	23	0.10	−1.17	0.10	n.s.			
MA	Ambient	24	−0.20	0.00	0.30	<0.05	<0.1 (i)	n.s.	n.s.
	Warm	24	−0.27	0.51	0.41	<0.01			
				Coefficient of variation (CV)					
SA	Ambient	28	−0.01	0.88	0.00	n.s.	n.s.	n.s.	<0.05
	Warm	28	0.03	0.92	0.05	n.s.			
MA	Ambient	28	−0.01	1.38	0.00	n.s.	<0.05 (s)	n.s.	<0.001
	Warm	28	0.10	1.17	0.23	<0.01			
LA	Ambient	20	−0.24	2.54	0.15	<0.1	n.s.	n.s.	<0.05
	Warm	20	−0.04	1.89	0.00	n.s.			
				Temporal mean relative biomass					
SA	Ambient	28	−0.05	0.62	0.32	<0.01	<0.05 (i)	<0.05	<0.01
	Warm	28	−0.05	0.79	0.38	<0.001			

Table 2 continued

Plankton group	Treatment	Linear regression					°C (Juliano's test)	°C (Wilcoxon's rank sum test)	
		N	Slope (*s*)	Intercept (*i*)	R^2	*P* value	*P* value	*P* value	
								Low-light	High-light
MA + LA	Ambient	28	0.05	0.38	0.32	<0.01	<0.05 (i)	<0.05	<0.01
	Warm	28	0.05	0.21	0.38	<0.001			

Plankton group	Treatment	Non-linear regression					°C	°C (Wilcoxon's rank sum test)	
		N	Half-saturation constant (h)	Maximum (m)	Factor	*P* value	*P* value	*P* value	
								Low-light	High-light
				Maximum biomass					
MA	Ambient	28	0.73	4.63		<0.001	<0.001 (h) <0.1 (m)	<0.05	<0.05
	Warm	28	1.35	4.83		<0.001			
				Relative biomass at peak time					
SA	Ambient	28			0.46	<0.001	<0.001	<0.05	n.s.
	Warm	28			0.89	<0.001			
MA + LA	Ambient	28	0.31	2.04		<0.001	<0.001 (h) <0.01(m)	<0.05	n.s.
	Warm	28	0.94	2.20		<0.001			

The last three columns show the significance of the temperature effect on these relationships for the entire light-spectrum (column 8), and low-light (column 9) and high-light conditions (column 10). s (slope), i (intercept), m (maximum) and h (half-saturation constant)

growth potential of MA and LA compared to SA at high-light conditions.

Primary production to biomass ratio

In the low-light experiments, the *P*/*B* increased with increasing light intensity at the beginning of the experiments (Fig. 4). During the bloom, it remained at a moderate level in 2005 (Fig. 4a, c) and slightly decreased in 2007 before the onset of nutrient depletion, probably due to self-shading (Fig. 4b, d). These results give an additional indication that nutrient depletion did not play a major role in the breakdown of the phytoplankton bloom in the low-light experiments.

In contrast, the *P*/*B* ratio strongly decreased by about 90 % during the bloom, parallel with increased self-shading and species shifts within and between the phytoplankton size groups in high-light conditions (Fig. 5). After the phytoplankton bloom, the *P*/*B* remained low in almost all high-light experiments (Fig. 5).

Food web structure and top-down control under ambient-temperature conditions

In almost all low-light experiments, the algal bloom was delayed probably due to a combination of low light and high initial biomasses of micro- and mesozooplankton (Figs. 4, 5). Zooplankton biomass followed the increase in phytoplankton biomass in all treatments (Fig. 4, 5). Probably due to strong light limitation of phytoplankton, the negative effect of consumers on phytoplankton biomass was less clear in the low-light than in high-light experiments (Figs. 6, 7).

Small-sized phytoplankton (SA)

The biomass of small-sized algae (SA) and edible microzooplankton (EMZ) was tightly coupled and showed predator–prey cycles in all experiments (Figs. 4, 5). In the high-light experiments 2008 and 2009, we found a distinct trophic cascade from copepods (COP) over EMZ to SA (Table 3; Figs. 6a, d, f, 7a, d, f), where the mean biomass of SA was negatively correlated with the mean biomass of EMZ and positively related to the mean biomass of COP. In addition, the mean biomass of EMZ was negatively correlated with the mean biomass of COP. Further indications of strong effects of grazers on SA are the high grazing pressure index (GPI_{SA}) in the high-light experiment 2009 (0.53 ± 0.17, median ± mad; $N = 6$) and the relatively low coefficient of variation (CV) of SA biomass (0.86 ± 0.24, mean ± SD; $N = 28$) across all experiments (Table 2; Fig. 8d). In the high-light experiments average

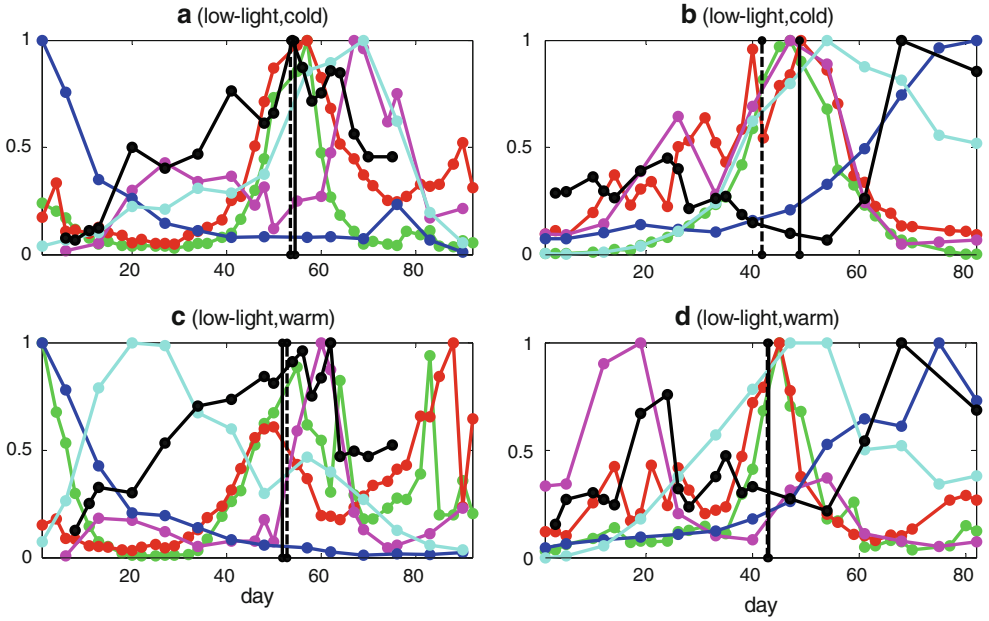

Fig. 4 The temporal dynamics of the biomasses of small-sized algae (*red*), medium-sized algae (*light-green*), copepods (*blue*), nauplii larvae (*cyan*), edible microzooplankton (*magenta*) and the primary production-to-biomass ratio (*P*/*B*) of the whole phytoplankton community (*black*) standardized for each group with its own maximum value and averaged over the cold ($\Delta T = 0$ °C, $\Delta T = 2$ °C, **a**, **b**)- and warm ($\Delta T = 4$ °C, $\Delta T = 6$ °C, **c**, **d**)-temperature treatments, in the low-light experiments 2005 (**a**, **c**) and 2007 (**b**, **d**). *Vertical lines* represent the onset of potential phosphorus (*solid*) and silicate (*dashed*) depletion

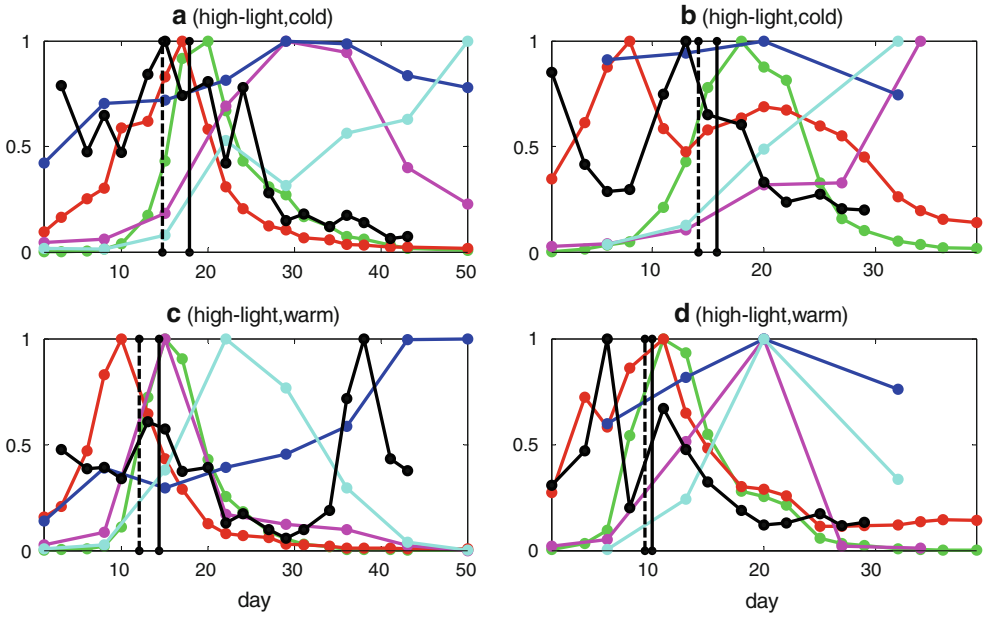

Fig. 5 The temporal dynamics of the biomasses of small-sized algae (*red*), medium-sized algae (*light-green*), copepods (*blue*), nauplii larvae (*cyan*), edible microzooplankton (*magenta*) and the primary production-to-biomass ratio (*P*/*B*) [d^{-1}] of the whole phytoplankton community (*black*) standardized for each group with its own maximum value and averaged over the cold ($\Delta T = 0$ °C, **a**, **b**)- and warm ($\Delta T = 6$ °C, **c**, **d**)-temperature treatments, respectively, for the high-light experiments 2008 (**a**, **c**) and 2009 (**b**, **d**). *Vertical lines* represent the onset of potential phosphorus (*solid*) and silicate (*dashed*) depletion

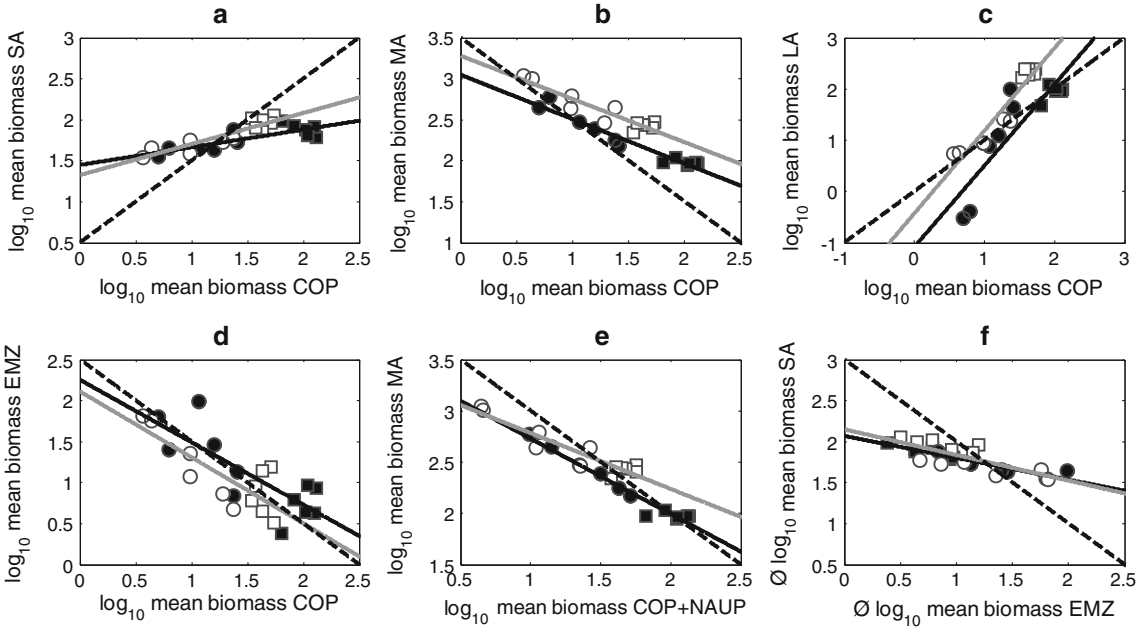

Fig. 6 Mean biomasses [μg C L^{-1}] of small-sized (SA, **a**), medium-sized (MA, **b**) and large-sized algae (LA, **c**), and edible microzooplankton (EMZ, **d**) in relation to the mean biomass [μg C L^{-1}] of copepods (COP) in the high-light experiments 2008 (*squares*) and 2009 (*circles*). **e** Mean biomass of MA in relation to summed mean biomasses of COP and nauplii. **f** Mean biomass of SA in relation to the mean biomass of EMZ. *White squares* indicate data from the ambient ($\Delta T = 0$ °C)- and *black squares* from the warm-temperature treatments ($\Delta T = 6$ °C). *Grey* ($\Delta T = 0$ °C) and *black* ($\Delta T = 6$ °C) *lines* represent significant ($P < 0.05$) linear regression *lines*. *Dashed lines* represent 1:1 relationships

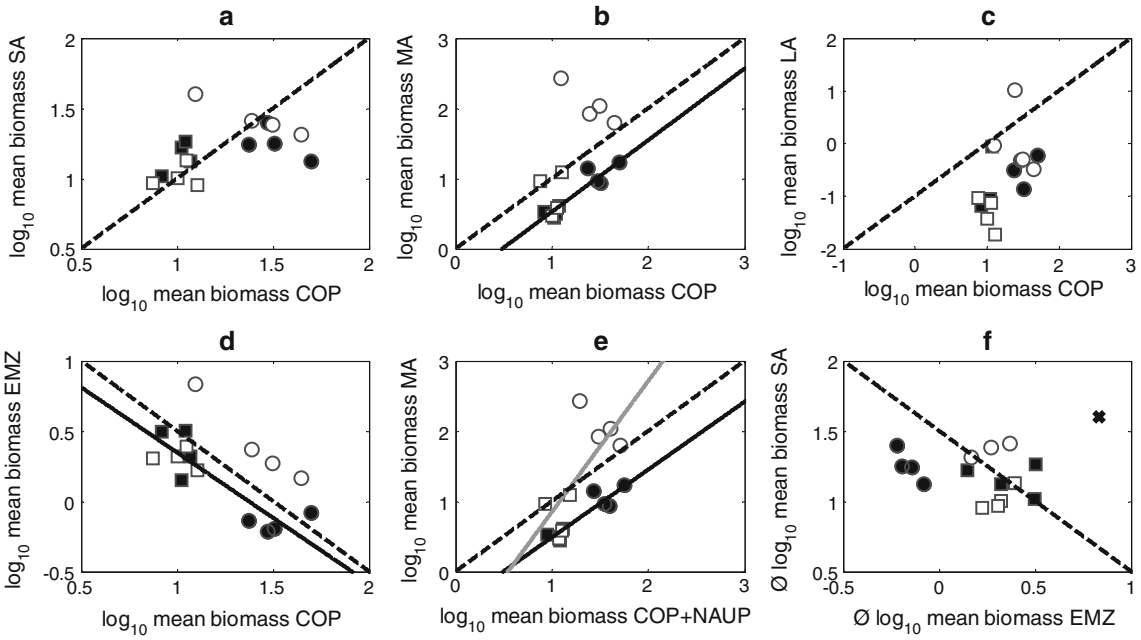

Fig. 7 Mean biomasses [μg C L^{-1}] of small-sized (SA, **a**), medium-sized (MA, **b**) and large-sized algae (LA, **c**), and edible microzooplankton (EMZ, **d**) in relation to the mean biomass [μg C L^{-1}] of copepods (COP) in the low-light experiments 2005 (*squares*) and 2007 (*circles*). **e** Mean biomass of MA in relation to summed mean biomasses of COP and nauplii. **f** Mean biomass of SA in relation to the mean biomass of EMZ. *White squares* indicate data from the ambient ($\Delta T = 0$ °C, $\Delta T = 2$ °C)- and *black squares* from the warm-temperature treatments ($\Delta T = 4$ °C, $\Delta T = 6$ °C). *Grey* ($\Delta T = 0$ °C, $\Delta T = 2$ °C) and *black* ($\Delta T = 4$ °C, $\Delta T = 6$ °C) *lines* represent significant ($P < 0.05$) linear regression *lines*. *Dashed lines* represent 1:1 relationships. Cross-marked values were excluded from calculations

Table 3 Results of linear regressions relating mean biomasses of small- (SA), medium- (MA) and large-sized algae (LA), copepods (COP), nauplii (NAUP), edible microzooplankton (EMZ), smaller (CS) and larger ciliates (CL) and heterotrophic dinoflagellates (DINO) to each other, separately for ambient (ΔT=0 °C, ΔT=2 °C) and warm (ΔT=4 °C, ΔT=6 °C) temperature treatments

Variables	Treatment	Linear regression					°C (Juliano's test)	°C (Wilcoxon's rank sum test)	
		N	Slope (*s*)	Intercept (*i*)	R^2	*P* value	*P* value	*P* value	
								Low-COP	High-COP
				High-light					
SA(COP)	Ambient	12	0.38	1.32	0.81	<0.001	<0.06 (s)	n.s.	n.s.
	Warm	12	0.22	1.45	0.64	<0.01			
MA(COP)	Ambient	12	−0.53	3.28	0.87	<0.001	<0.06 (i)	<0.1	<0.01
	Warm	12	−0.54	3.05	0.94	<0.001			
LA(COP)	Ambient	12	1.61	−0.43	0.90	<0.001	n.s.	n.s.	<0.01
	Warm	12	1.59	−1.09	0.78	<0.001			
EMZ(COP)	Ambient	12	−0.80	2.12	0.64	<0.01	n.s.	n.s.	n.s.
	Warm	12	−0.76	2.26	0.65	<0.01			
MA(COP + NAUP)	Ambient	12	−0.55	3.33	0.88	<0.001	<0.05 (s)	–	–
	Warm	12	−0.73	3.47	0.96	<0.001			
SA(EMZ)	Ambient	12	−0.31	2.15	0.56	<0.01	n.s.	–	–
	Warm	12	−0.27	2.07	0.88	<0.001			
CS(COP)	Ambient	12	−0.88	1.97	0.54	<0.01	n.s.	n.s.	n.s.
	Warm	12	−0.56	1.67	0.75	<0.001			
CL(COP)	Ambient	12	−1.70	2.07	0.82	<0.001	n.s.	n.s.	n.s.
	Warm	12	−1.49	2.01	0.81	<0.001			
DINO(COP)	Ambient	12	−0.27	0.89	0.18	n.s.	<0.1 (i)	n.s.	n.s.
	Warm	12	−0.83	1.91	0.47	<0.05			
				Low-light					
SA(COP)	Ambient	8	0.50	0.62	0.31	n.s.	n.s.	n.s.	n.s.
	Warm	8	0.15	1.02	0.13	n.s.			
MA(COP)	Ambient	8	1.62	−0.55	0.37	n.s.	n.s.	n.s.	<0.05
	Warm	8	1.02	−0.49	0.87	<0.001			
LA(COP)	Ambient	8	1.71	−2.71	0.28	n.s.	n.s.	n.s.	n.s.
	Warm	8	0.83	−1.71	0.29	n.s.			
EMZ(COP)	Ambient	8	−0.25	0.66	0.11	n.s.	<0.05 (s)	n.s.	<0.05
	Warm	8	−0.93	1.28	0.75	<0.01			
MA(COP + NAUP)	Ambient	8	1.86	−1.01	0.51	<0.05	n.s.	–	–
	Warm	8	0.97	−0.48	0.85	<0.01			
SA(EMZ)	Ambient	7	−0.06	1.18	0.00	n.s.	n.s.	–	–
	Warm	8	−0.21	1.23	0.31	n.s.			
CS(COP)	Ambient	8	0.06	−0.09	0.05	n.s.	<0.01 (s) <0.05 (i)	n.s.	<0.05
	Warm	8	−0.42	0.35	0.87	<0.001			
CL(COP)	Ambient	8	−0.49	0.71	0.12	n.s.	<0.05 (s) <0.1 (i)	n.s.	<0.05
	Warm	8	−1.91	2.05	0.68	<0.05			
DINO(COP)	Ambient	8	−0.21	−0.50	0.07	n.s.	n.s.	n.s.	n.s.
	Warm	8	0.28	−1.46	0.06	n.s.			

The last three columns show the significance of the temperature effect on these relationships for the entire copepod biomass-spectrum (column 8), and low copepod (column 9) and high copepod biomasses (column 10). Results of column 9 (10) represent the significance of the difference between the gray and black lines on Fig. 7 (6). s (slope) and i (intercept)

CV of MA (1.37 ± 0.21; $N = 20$) and LA (1.31 ± 0.53; $N = 20$) were both significantly higher (Wilcoxon's rank sum test, $P < 0.001$, MA, $P = 0.001$, LA) than that of SA (0.84 ± 0.27; $N = 20$), which they exceed by a factor of 1.6. Similarly, the mean CV of MA (1.32 ± 0.28; $N = 8$) was 1.5 (Wilcoxon's rank sum test, $P = 0.003$) times

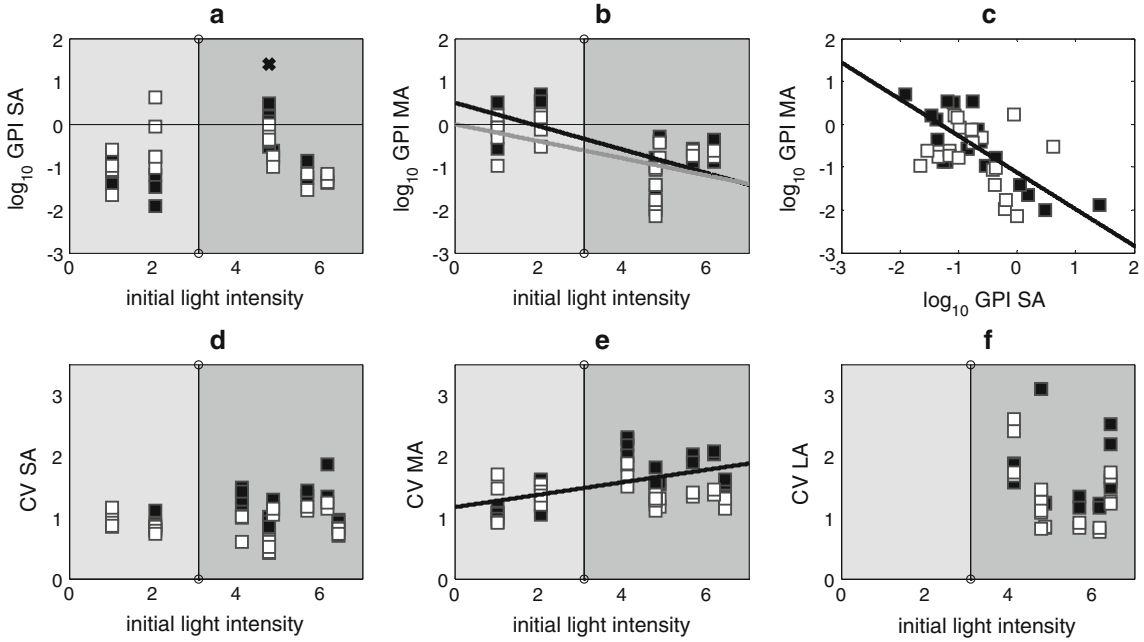

Fig. 8 Grazing pressure index (GPI, **a**, **b**) and the coefficient of variation (CV) (**d**–**f**) of the small-sized algae (SA, **a**, **d**), medium-sized algae (MA, **b**, **e**) and large-sized algae (LA, **f**) biomasses in relation to the initial light intensity [Watt $m^{-2}d^{-1}$] of the experiments. The GPI for SA (GPI_{SA}) and MA (GPI_{MA}) at their particular peak time were calculated according to the formula $GPI_{SA} = (EMZ + IMZ)\cdot(PP\cdot(SA \cdot PC^{-1}))^{-1}$ and $GPI_{MA} = (EMZ + IMZ) \cdot (PP \cdot (MA\cdot PC^{-1}))^{-1}$ where SA and MA are the small- and medium-sized algae biomasses, EMZ and IMZ are the edible and inedible microzooplankton biomasses, COP and NAUP are the copepod and nauplii biomasses, PC and PP are the biomass and the measured primary production of the total phytoplankton community. The CV (standard deviation divided by mean) was calculated for the time series of the biomass of the different phytoplankton size groups in the mesocosms. **c** The GPI_{SA} in relation to GPI_{MA}. *White squares* indicate data from the cold ($\Delta T = 0$ °C, $\Delta T = 2$ °C)- and *black squares* from the warm-temperature treatments ($\Delta T = 4$ °C, $\Delta T = 6$ °C). Low-light and high-light experiments are marked *light* and *dark grey*, respectively. *Grey* ($\Delta T = 0$ °C, $\Delta T = 2$ °C) and *black* ($\Delta T = 4$ °C, $\Delta T = 6$ °C) *curves* represented significant ($P < 0.05$) linear regression lines. *Cross-marked* values were excluded from calculations

higher than that of SA (0.89 ± 0.14; $N = 8$) in the low-light experiments. These results indicate a stronger top-down control of SA compared to MA and LA independent of light levels. However, GPI_{SA} values were low in the experiments 2005–2008 regardless of light levels (0.10 ± 0.59, median ± mad; $N = 14$) (Table 2; Fig. 8a).

Medium- (MA) and large-sized phytoplankton (LA)

The dynamics of medium-sized algae (MA) and nauplii and copepods (COP) were tightly coupled (Fig. 4, 5). In addition, the mean biomass of MA was negatively correlated with the mean biomass of COP in the high-light experiments 2008 and 2009 (Table 3; Fig. 6b) suggesting a pronounced top-down control of MA. The impact of top-down processes on the dynamics of MA depended on light intensity (Table 2; Fig. 8). GPI_{MA} at peak time was much higher in the low-light (0.80 ± 0.50, median ± mad; $N = 8$) than in the high-light experiments (0.09 ± 0.13, median ± mad; $N = 12$) (Table 2; Fig. 8b), indicating reduced top-down control of MA at high-light conditions.

In addition, the mean biomasses of LA and COP were positively correlated in the high-light experiments (Table 3; Fig. 6c), suggesting a predator-mediated release of LA from competition with MA.

Microzooplankton (MZ)

The various microzooplankton groups showed different responses to altered abiotic and biotic conditions. The maximum biomasses of smaller ciliates and heterotrophic dinoflagellates increased with increasing initial light intensity, whereas the maximum biomass of larger ciliates decreased, resulting in hardly any response of the maximum biomass of the entire edible microzooplankton group (EMZ) to light (Table 2; Appendix 4). The biomass of larger ciliates decreased more pronouncedly with increasing copepod biomass than that of smaller ciliates and heterotrophic dinoflagellates (Table 3; Appendix 3), indicating a preference of copepods for larger ciliates.

The inedible microzooplankton (IMZ) was negatively correlated with heterotrophic dinoflagellates across all experiments (Appendix 4) (linear regression: $R^2 = 0.77$, $P < 0.001$, $N = 14$), suggesting intraguild predation within microzooplankton. In addition, heterotrophic dinoflagellates were rare in the low-light experiments but reached

high maximum biomasses (8 ± 5 ìg C L^{-1}; $N = 12$) in the high-light experiments 2008 and 2009 (Table 2; Appendix 4). This indicates food limitation of heterotrophic dinoflagellates in the low-light treatments.

The influence of temperature on bottom-up and top-down regulation

Small- (SA) and large-sized phytoplankton (LA)

SA and LA responded very little to increasing temperature (Tables 2, 3). The biomass dynamics of EMZ followed that of SA with shorter time lags in the warmer treatments, indicating a stronger top-down control at higher temperature (Figs. 4, 5). However, the biomass of EMZ and thus top-down control on SA was reduced by temperature at the combination of high copepod biomasses and low light (Table 3; Fig. 7d; Appendix 3). The bottom-up control of SA and LA by nutrients also hardly changed (Table 1).

Medium-sized phytoplankton (MA)

The effect of temperature on the regulation of MA depended on light levels. At low-light conditions, warming negatively affected the maximum biomass of MA (Table 2; Fig. 3b) and strengthened the coupling of MA and mesozooplankton biomass (Fig. 4), indicating an enhanced top-down control. At the same time, the timing of nutrient depletion, CV and mean net growth rate remained mostly unaffected by temperature increase (Tables 1, 2).

In the high-light experiments, increased temperature enhanced the effect of both top-down and bottom-up factors on MA. Increased temperature had a negative effect on both the maximum and mean biomass of MA (Tables 2, 3; Figs. 3b, 6b, e), but the latter was only marginally significant ($P < 0.1$). The negative effect of temperature on MA biomass was presumably due to stronger grazing by copepods as well as their enhanced reproduction and subsequent grazing by nauplii. This assumption is based on the result that the summed biomass of COP and nauplii explained a higher share of the variance of MA than the biomass of adult COP alone (Table 3; Fig. 6e) and by a positive temperature effect on the biomass maximum of the nauplii at high-light conditions (Table 2; Appendix 4). One indication of enhanced bottom-up regulation at increased temperature is the higher CV of the biomass of MA in the warm treatments (Table 2, Fig. 8e). In addition, in the high-light experiments, the mean net growth rate of MA was higher in the warm (1.60 ± 0.14 d^{-1}, $N = 20$) than in the cold treatments (1.43 ± 0.10 d^{-1}, $N = 20$) (Table 2; Fig. 3e). Nutrient depletion occurred earlier in the warmer treatments of the high-light experiments for all nutrients (Wilcoxon's rank sum test, $N_1 = 16$, $N_2 = 16$, $P = 0.01$, respectively for N, P and Si). Furthermore, we observed a reduced time lag between the date of MA biomass maximum and the onset of phosphorus depletion (Table 1; Fig. 2).

Microzooplankton (MZ)

The negative relation between IMZ and the heterotrophic dinoflagellates across all experiments (Appendix 4) was less pronounced in the warm treatments (linear regression: $R^2 = 0.41$, $P < 0.01$, $N = 16$). Heterotrophic dinoflagellates reached very high maximum biomasses (153 ± 208 ìg C L^{-1}; $N = 4$) in the warm treatments of the high-light experiments 2009 at low and moderate copepod biomasses (Table 2; Appendix 3).

Development and composition of the phytoplankton community

The phytoplankton community was dominated by MA and LA during the bloom in almost all experiments (Fig. 9b). The relative biomass of SA during the bloom and the entire experiment strongly decreased with increasing initial light intensity (Table 2; Fig. 9). Temperature had a positive impact on the relative contribution of SA (Table 2; Fig. 9).

Discussion

In general, the biomass peak of phytoplankton occurs when its light- and nutrient-dependent gross growth equals the summed losses by respiration, sedimentation and grazing (Thackeray et al. 2008; Wiltshire et al. 2008). Two mechanisms may terminate positive net growth: decline of the growth rate due to nutrient depletion and/or self-shading (light limitation) or increase in the loss rates because of higher grazing, sedimentation and/or flushing (Reynolds 2006, Thackeray et al. 2008). We observed both mechanisms in our study system. According to our hypotheses, the dominance of one or the other mechanism depended on cell size. Consequently, the effects of warming differed between size groups and were modified by light intensity. This provides an explanation for the different responses of phytoplankton to climate change observed at regional scales.

Size-dependent regulation of phytoplankton under ambient-temperature conditions

Small-sized phytoplankton (SA)

We observed low SA biomasses throughout the experiments. Our analyses suggest that this was most likely due

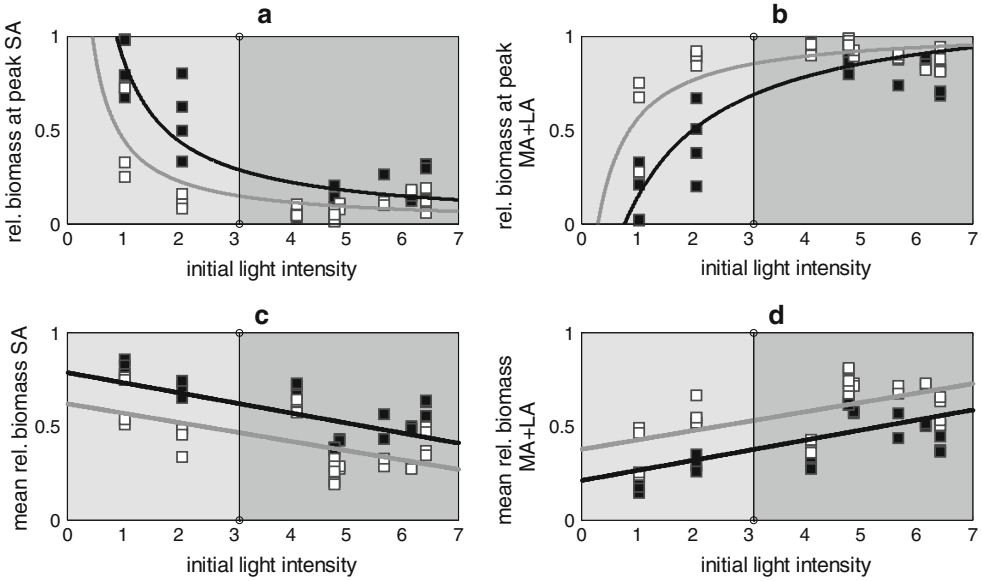

Fig. 9 The relative contributions of small-sized (SA, **a**, **c**) and summed medium- (MA) and large-sized (LA) algae (**b**, **d**) biomasses at the day of the peak of the entire phytoplankton community (**a**, **b**) and averaged over the whole experiment (**c**, **d**) in relation to the initial light intensity [Watt $m^{-2}d^{-1}$] of the experiments. *White squares* indicate data from the ambient ($\Delta T = 0$ °C, $\Delta T = 2$ °C)- and *black squares* from the warm-temperature treatments ($\Delta T = 4$ °C, $\Delta T = 6$ °C). *Grey* ($\Delta T = 0$ °C, $\Delta T = 2$ °C) and *black* ($\Delta T = 4$ °C, $\Delta T = 6$ °C) *curves* represented significant ($P < 0.05$) linear and non-linear regression *lines*

to ciliate grazing, in agreement with H1(1). The biomass maximum and mean net growth rate of SA increased only weakly with increasing initial light intensity (Table 2; Fig. 3a, d). Even under high-light conditions, SA biomasses remained relatively low in our experiments, probably as they were immediately consumed, resulting in high biomasses of smaller and partly also of larger ciliates (Appendix 4). The timing of the SA biomass peak was not related to the onset of nutrient depletion (Table 1; Fig. 2a, d), which indicated only a minor role of nutrient limitation in the breakdown of the SA bloom. SA biomass was less variable in time than the biomasses of MA and LA (Table 2; Fig. 8d–f). This suggests that density-dependent loss processes such as grazing by ciliates already affected the biomass of SA when it was relatively low, resulting in an early predator-mediated breakdown of the SA bloom. This assumption is supported by a tight coupling of the dynamics of SA and EMZ (dominated by ciliates) (Figs. 4, 5). EMZ biomass strongly increased in the experiment 2008 after the peak of SA biomass (Fig. 5a, c). The SA grazing pressure index was high at the SA peak time in the experiment 2009 but low otherwise (Fig. 8a). In the low-light experiments, the mean net growth rate of SA was very low (Fig. 3d) and thus a small grazing pressure of EMZ was presumably enough to break down their bloom. Due to their similar maximum growth rates, smaller phytoplankton cannot outgrow ciliates (Smith and Lancelot 2004; Vadstein et al. 2004; Irigoien et al. 2005). Strong top-down control of pico- (Smith and Lancelot 2004; Barber and Hiscock 2006; Horn and Horn 2008) and nanophytoplankton (Smith and Lancelot 2004; Irigoien et al. 2005) was found in other studies, including both field and experimental works.

Medium- (MA) and large-sized phytoplankton (LA)

Confirming H1(2), MA and LA were predominantly influenced by the abiotic forcing regime, especially by light. Biomass maxima and mean net growth rates strongly increased with increasing initial light intensity (Table 2; Fig. 3b, c, e, f). At high light, MA strongly increased until nutrient limitation and, to a smaller extent, self-shading resulted in the breakdown of the MA bloom. In the high-light experiments, the peak time of MA was related to nutrient depletion (Table 1; Fig. 2b), and the *P*/*B* ratio strongly decreased during and after the bloom (Fig. 5). The decline in *P*/*B* may be partly related to species shifts towards more competitive (with higher nutrient affinity and/or storage capacity) but slow-growing phytoplankton after nutrient depletion.

The dynamics of mesozooplankton and MA were strongly coupled (Fig. 5), and MA and copepod biomasses were negatively related (Fig. 6b, e). However, grazing pressure was low at the peak time of MA in the high-light experiments (Fig. 8b), probably as copepod biomasses remained low despite abundant prey, as copepods cannot track changes in food supply quickly due to their complex life cycle and long development time (Calbet 2008). Thus, losses from grazing were probably less important than the decrease in production due to competition for nutrients (Sommer and Lewandowska 2011; own results), light limitation/self-shading (own results) and sedimentation (Wohlers et al. 2009). Phytoplankton tend to aggregate during the positive net growth period in seasonal spring, especially when densities are high and nutrients are depleted (Lundsgaard et al. 1999). Our results support the 'loophole' hypothesis of Irigoien et al. (2005) according to which good nutrient and light conditions open a possibility for phytoplankton species to escape predation

and build up high biomass until the nutrient-limited bloom collapses if they are defended against microzooplankton grazing and their growth rates strongly exceed those of their mesozooplankton grazers. Strong regulation of microphytoplankton by abiotic forcing factors was also reported in other experiments, such as by light (Bramm et al. 2009) or nutrients (Smith and Lancelot 2004; Vadstein et al. 2004; Sinistro 2010) in mesocoms (Vadstein et al. 2004), in lakes (Bramm et al. 2009; Sinistro 2010) and in marine systems (Smith and Lancelot 2004).

In contrast to the high-light experiments, we found no clear relationship between the peak time of MA and the onset of nutrient depletion in the low-light experiments (Table 1; Fig. 2e). This suggested that the low-light intensities did not allow sufficient increase in the phytoplankton biomass to deplete the available nutrients. This assumption is supported by Sommer et al. (2007) who showed that the phytoplankton community was only moderately P-limited in the experiment 2005 (low-light) during their bloom. As the net- and most likely also the gross growth rate of the medium-sized phytoplankton was low (Fig. 3e, initial light intensities of 1.03 and 2.06 Watt $m^{-2}d^{-1}$), a small increase in grazing pressure was enough to end the positive net growth period, that is, to break down the bloom. This is supported by a tight coupling of mesozooplankton and MA dynamics (Fig. 4) and a very high grazing pressure at the peak time of MA in the low-light experiments (Table 2; Fig. 8b). Altered nutrient concentrations and light intensities also had strong influences on the dynamics of LA. This group was rare in the low-light experiments but achieved higher biomasses in the high-light experiments (Table 2; Fig. 3c) where their peak time was related to the onset of nutrient depletion (Table 1; Fig. 2c). We also observed a positive relation between LA and copepods (Table 3; Fig. 6c). This is probably due to the release of LA from competition with MA for nutrients and light. A similar mechanism was proposed to explain the significant increase in large diatoms such as *Coscinodiscus wailesii* and *Guinardia delicatula* in the North Sea (Wiltshire et al. 2010).

Indirect trophic effects under ambient temperature

It is generally known that copepods may promote the growth of small-sized algae (SA) by feeding on their consumers, such as ciliates (Vincent and Hartmann 2001; Jakobsen et al. 2005; Sommer and Sommer 2006), thus reducing their grazing pressure on SA (Vadstein et al. 2004; Stibor et al. 2004; Sommer et al. 2005a; Sommer and Sommer 2006; Zöllner et al. 2009). This was also observed in our system, indicated by the positive relation between copepods and SA (Table 3; Fig. 6a), and the negative relation between copepods and edible microzooplankton (EMZ) and between EMZ and SA (Table 3; Fig. 6d, f). However, the positive relation between copepods and SA may also be partly attributed to reduced competition between SA and MA for nutrients and light (Fig. 1, McCauley and Briand 1979; Irigoien et al. 2005), as MA are themselves strongly grazed by copepods (Table 3; Fig. 6b, e). The negative relation between copepods and EMZ may also be partly related to their enhanced competition for nano- (Ptacnik et al. 2004) and microphytoplankton (Vadstein et al. 2004; Aberle et al. 2007; Löder et al. 2011a, b). This holds most likely for the heterotrophic dinoflagellates, since these are less-preferred prey for copepods (Vincent and Hartmann 2001; Jakobsen et al. 2005 but see also Kleppel 1993; Ptacnik et al. 2004). Although large ciliates overlap with copepods in their dietary spectra (Aberle et al. 2007), their negative relation may be predominately attributed to increased grazing pressure, as they are often strongly grazed by copepods (Zöllner et al. 2003; Vincent and Hartmann 2001; Jakobsen et al. 2005).

Although we found a positive relationship between SA and copepods in the high-light experiments, the increase in SA biomass with copepod biomass was small. This might be due to the release of heterotrophic nanoflagellates (HNF), that is, predators of SA (Sommer 2005), from predation by ciliates at high copepod biomass. This assumption is supported by the results of Zöllner et al. (2003, 2009). In their experiments, the density of copepods was negatively correlated with the density of ciliates and positively correlated with the density of heterotrophic and autotrophic nanoflagellates. We did not find a clear relationship between the mean SA biomass and the mean EMZ and copepod biomasses in the low-light experiments (Fig. 7a, f). This may be related to compensatory effects due to different responses of pico- and nanophytoplankton (see below) but also to the fact that the low-light experiments were longer than the high-light experiments; thus, the bloom conditions (when predator–prey relationships are most pronounced) affected mean biomasses less.

Warming-induced changes in the relative importance of bottom-up and top-down factors depend on cell size and light intensity

Small-sized phytoplankton (SA)

As rising temperatures accelerated the metabolism of micro- and mesozooplankton equally (Rose and Caron 2007), we expected that increased grazing of EMZ on SA is counteracted by increased copepod grazing on ciliates and by release from competition with medium-sized algae for nutrients. Thus, we anticipated little influence of increased temperature on the biomass of SA—H2(1). This expectation was largely confirmed by our analysis (Tables 2, 3; Figs. 3a, 6a, 7a).

We identified several, complex indirect food web interactions affecting the biomass of SA. We observed a stronger

coupling of the dynamics of SA and EMZ at increased temperature (Figs. 4, 5), without a decrease in SA biomass or an increase in the biomass maximum of EMZ (Appendix 4). The latter was probably due to increased grazing on EMZ by copepods (Fig. 6d). In addition, different responses of pico- and nanophytoplankton, here aggregated into SA, may have counteracted each other (Lewandowska and Sommer 2010). In the high-light experiment 2008 at high copepod biomass, picophytoplankton biomass maximum was higher in the warm- than in the ambient-temperature treatments. Thus, the lack of a temperature effect on the whole SA group in this experiment could only arise from a negative response of nanophytoplankton to elevated temperature. Furthermore, in the high-light treatments, the biomass of larger ciliates was low, presumably due to a pronounced grazing by copepods, whereas the biomass of smaller ciliates reached very high biomasses at both temperature treatments (Appendix 3, 4), suggesting a high grazing pressure on nanophytoplankton and most likely also on HNF. The latter presumably led to the increase in picophytoplankton biomass at elevated temperature (Lewandowska and Sommer 2010). In contrast, increased HNF grazing on SA might be responsible for the absent temperature effect on SA in the warmer treatments of the experiment 2007, which could be otherwise expected as ciliate biomass strongly decreased at elevated temperature (Table 3; Fig. 7a, d). The latter is associated with high biomasses and increased grazing rates of copepods in the warmer treatments.

The absence of a temperature effect on SA could also be due to a too narrow temperature range in the experiments. Even if a very high Q_{10}-value of 6.5 is assumed for the temperature-sensitive ingestion rate of copepods (Isla et al. 2008), an increase in temperature by 6°C is similar to a tripling of copepod biomass, which is lower than the variation in copepod biomasses throughout the experiments, ranging over almost two orders of magnitude. Other reasons might be a shift in species composition within the SA group in time, enhanced respiratory losses of SA accompanied by a release of SA from competition with MA and/or increased intraguild predation within the microzooplankton as it is indicated by the negative relation between inedible microzooplankton (IMZ) and heterotrophic dinoflagellates (Appendix 4). Heterotrophic dinoflagellates prey upon both phytoplankton and ciliates (Tillmann 2004).

Medium-sized phytoplankton (MA)

In agreement with H2(2), our results indicate that the lower biomass of MA observed at elevated temperatures (Tables 2, 3; Figs. 3b, 6b) was caused by higher grazing and enhanced reproduction of mesozooplankton (Figs. 4, 5, 6b, e) and thus higher top-down control, in line with the findings of Gaedke et al. (2010) and Sommer and Lewandowska (2011). However, the strong decrease in MA biomass at elevated temperatures may be attributed not only to enhanced mesozooplankton grazing (Sommer and Lewandowska 2011) but also to enhanced grazing by heterotrophic dinoflagellates. These reached considerably higher biomasses in some of the warm treatments, especially when copepod biomass was low (Appendix 3, 4). The decrease in the MA mean biomass with increasing mean biomass of copepods was small compared to the strong temperature effect (Fig. 6b). This might be due to indirect trophic effects since copepods may affect MA negatively by direct consumption (COP → MA) but also positively via grazing on microzooplankton (COP → EMZ → MA). Higher sedimentation (Piontek et al. 2009) and respiration rates (Wohlers et al. 2009) might also contribute to the lower biomasses of MA at elevated temperatures, as higher temperatures increase the aggregation potential of diatom cells (Piontek et al. 2009) and accelerate heterotrophic processes.

Overall, we found complex interactions between abiotic and biotic factors determining the response of phytoplankton groups to warming. Increased temperature may lead to reduced phytoplankton biomass due to higher zooplankton grazing and to earlier nutrient depletion (own results) besides higher sedimentation losses and lower nutrient supply caused by earlier and stronger stratification (Wohlers et al. 2009). This fits with the warming-associated global decrease in chlorophyll in the past 100 years (Boyce et al. 2010). However, the increased windiness in early spring as expected for the Baltic Sea area (Lehmann et al. 2011) may reduce water column stability (by increasing vertical mixing) and phytoplankton sinking losses, this way counteracting the abovementioned negative temperature effects on phytoplankton. Other climate change–related alterations such as altered cloudiness (BACC 2008; Lehmann et al. 2011) might also influence phytoplankton growth and mortality. In addition, the impact of warming on phytoplankton in oceans may differ between cooler and warmer waters (Richardson and Schoeman 2004; Boyce et al. 2010).

Overall, our results suggest that in combination with less available light due to increased cloudiness, as anticipated for the southern Baltic Sea (BACC 2008), climate change may lead to less net sequestration of atmospheric CO_2. This likely implies less carbon export to deeper regions of oceans and a lower food supply for heterotrophs, which may result in altered trophic interactions and community structures (Duffy and Stachowicz 2006; O'Connor et al. 2009; Wiklund et al. 2009).

Interestingly, warming-induced changes in the relative importance of bottom-up and top-down factors differed between low-light and high-light experiments. At severe light limitation, elevated temperatures increased zooplankton grazing on MA (Table 2; Figs. 3b, 4). In contrast, algal gross growth was little accelerated by temperature under severe light limitation (Tilzer et al. 1986; Sommer 2005).

Nevertheless, we found no temperature effect on mean net growth rates (Table 2; Fig. 3e). The negative consequences of enhanced grazing for MA net growth may have been buffered by decreased self-shading due to the reduced MA biomass, which increases their *P*/*B*. The weak (2005) and strong (2007) positive temperature effects on *P*/*B* of the phytoplankton community during the positive growth phase of the phytoplankton in the low-light experiments (Lewandowska 2011) supports this assumption. The strong increase in *P*/*B* in 2007 could also be partly related to a change from light-limited to non-light-limited conditions. In contrast, at high-light conditions and thus weak influence of light, enhanced temperature increased not only zooplankton grazing (as indicated by the lower MA biomass and the tighter coupling of the MA and mesozooplankton dynamics (Tables 2, 3; Figs. 3b, 5, 6b) but also net (Table 2; Fig. 3e) and most likely gross growth rates of MA. This led to an earlier depletion of nutrients (Fig. 2b) at elevated temperatures. This assumption is additionally supported by the higher CV of MA and the tighter coupling of the MA and phosphorus dynamics at increased temperature (Tables 1, 2; Figs. 2, 8e). Therefore, the decrease in phytoplankton biomass due to warming could be counteracted by enhanced nutrient input from rivers in coastal areas (Wasmund et al. 2008; Neumann 2010).

Large-sized phytoplankton (LA)

In contrast to our expectations (H2(3)), the statistical results regarding the temperature effect on LA were inconsistent (Tables 2, 3; Figs. 3c, 6c), partly because LA were rare in most of the years. Reduced MA biomass coincided with reduced phytoplankton community biomass at increased temperature (Sommer and Lengfellner 2008; Lewandowska and Sommer 2010; Sommer and Lewandowska 2011). This probably decreased competition not only between LA and MA but also between all phytoplankton size groups. However, earlier nutrient depletion in the warmer treatments might have affected the rather slow-growing LA negatively. Thus, the positive effect of temperature (release from competition) was probably counteracted by its negative effect (earlier nutrient depletion), leading to no clear temperature effect on LA biomass (Table 2). Under natural conditions, additional effects of higher temperature may include increased sedimentation rates and lower nutrient concentrations due to earlier and stronger stratification and consequently more severe nutrient depletion.

Temperature-induced shifts in community composition

Our results suggest that climate change has hardly any influence on the biomass of small-sized algae (SA) and decreases the biomass of medium-sized algae (MA), resulting in a shift of the phytoplankton composition towards smaller cell sizes (Fig. 9). Hence, the increased share of SA at elevated temperature is an indirect consequence of reduced MA biomass and not of an enhanced SA biomass. This result is in line with the findings of Daufresne et al. (2009) (for 2005, 2006-2 and 2007), Lewandowska and Sommer (2010) (for 2008) and Sommer and Lewandowska (2011) (for 2009) where a decrease in mean cell and particle size of the mesocosm phytoplankton community at increased temperature was described during the individual experiments. A warming-induced shift towards smaller phytoplankton was also reported for experiments with freshwater phytoplankton (Yvon-Durocher et al. 2011), lakes (Winder et al. 2009) and estuaries (Guinder et al. 2010). The mechanisms behind the warming-induced shift in phytoplankton community towards smaller cell sizes differ between systems. They may be associated with higher zooplankton grazing on medium-sized algae, as in Ryther and Sanders (1980) and this study, higher sedimentation of larger phytoplankton (Piontek et al. 2009), or decreased nutrient concentrations as in Winder et al. (2009). The latter mechanism was presumably also relevant in our study. Nutrient depletion occurred earlier in the warmer treatments of the high-light experiments, which likely promotes small-sized algae as they have generally lower nutrient demands due to their favourable surface-to-volume ratio (Richardson 2008; Winder et al. 2009; Finkel et al. 2010; Litchman et al. 2010).

Besides temperature, light influenced the phytoplankton community composition as well. The share of SA decreased with increasing initial light intensity, whereas the share of MA and LA increased. Smaller phytoplankton has a growth advantage at strong light limitation due to its lower internal light shading (Finkel et al. 2010) and sinking rates compared to larger phytoplankton, except for large, but thin and needle-shaped species, which were not common in our experiments. A higher share of smaller phytoplankton at lower light intensities was also found in other experiments (Bramm et al. 2009).

Overall, our results suggest that the predicted higher temperature and lower light intensity under climate change in winter and early spring (IPCC 2007) will lead to an increase in the relative contribution of smaller phytoplankton in the Baltic Sea. Such changes in the phytoplankton community may have far-reaching consequences for the energy transfer to higher trophic levels and for the copepod community (Richardson 2008; Sommer and Lengfellner 2008).

We conclude that for giving reliable predictions about the effects of climate change on phytoplankton, we need to understand the direct and indirect interspecific interactions within the pelagic food web, and the influence of temperature and light on their strength. This task, although rendered difficult by the overwhelming complexity of natural food webs, is eased by a size-based grouping of species, which reflects their trophic interactions with other groups.

Summary

In the present study, we showed that phytoplankton size groups differ in their regulation, which has presumably implications for their responses to climate change. Warming strengthened predator–prey interactions. Climate change–related direct effects (as for example increased grazing of ciliates on SA) were counteracted by indirect effects through trophic cascading and altered competition structure. Increased grazing of ciliates (copepods) on HNF (ciliates) reduced grazing of HNF (ciliates) on SA. Different indirect effects may have been compensated by each other. Additionally, we identified light-dependent influences of warming on phytoplankton size groups. Our findings motivate to further investigate the indirect effects of climate change on food webs with emphasis on abiotic–biotic interactions and different size (functional) groups.

Acknowledgments This work was funded by the Deutsche Forschungsgemeinschaft (DFG) within the priority program 1162 'The impact of climate variability on aquatic ecosystems' (AQUASHIFT). Francisco de Castro is acknowledged for advice on computational issues. T. Klauschies also thanks Aleksandra Lewandowska for help in technical questions.

Appendix 1

See Table 4.

Table 4 Classification of autotrophic phytoplankton and microzooplankton into functional groups

Genus	Epitheton	Cell volume (μm^3)	Detected
Small-sized algae (SA)			
Chaetoceros	*minimum*	70	2005/06-1/06-2/07/08
Chrysochromulina	sp.	204	2005/07
Dinobryon	*balticum*	38	2005/06-1/06-2/08/09
Gymnodinium	*ostenfeldii*	400	2005/06-1/06-2/07/08
Gymnodium	sp.	187	2009
Heterocapsa	*rotundata*	430	2005/06-1/06-2/07/08/09
Heterocapsa	*cef*		2009
Plagioselmis	*prolonga*	66	2005/06-1/06-2/07/09
Pseudonitzschia	sp.	53	2005/06-1/06-2/07/08/09
Teleaulax	*amphioxeia*	990	2005/06-1/06-2/07/08/09
Tetraselmis	sp.	1,210	2006-1/06-20/07/08
Picoplankton	sp.	Changing	2005/06-1/06-2/07/08/09
Medium-sized algae (MA)			
Cerataulina	*pelagica*	40,000	2005/06-1/06-2/07/08
Chaetoceros	*curvisetus*	1,500	2005/06-1/06-2/07/08/09
Dictyocha	*speculum*	820	2007
Ditylum	*brightwellii*	28,000	2006-1/06-2
Guinardia	*delicatula*	5,130	2009
Gymnodinium	*lohmannii*	15,700	2005/06-1/06-2/07/08
Gyrodinium	*fusiforme*	28,300	2006-1/06-2/07/08
Navicula	sp.	720	2005/06-1/06-2/07
Nitzschia	*acicularis*	70	2005/06-1/06-2/07/08
Rhizosolenia	*alata*	37,700	2005/06-1/06-2/07/08/09
Rhodomonas	*marina*	2,300	2007/08/09
Skeletonema	*costatum*	100	2005/06-1/06-2/07/08/09
Tabularia	*fasciculata*	14,000	2005/06-1/06-2/2007
Thalassionema	*nitzschioides*	1,800	2005/06-1/06-2/07/08/09
Thalassiosira	*nordenskioeldii*	3,600	2005/06-1/06-2/07/08/09
Thalassiosira	*rotula*	42,250	2008/09
Scripsiella	sp.	22,449	2009
Pentapharsodinium	sp.	22,449	2009
Large-sized algae (LA)			
Ceratium	*fusus*	45,000	2006-1/06-2/09
Ceratium	*tripos*	60,000	2006/08/09
Coscinodiscus	sp.	1,960,000	2005/06-1/06-2/07/08
Odontella	*aurita*	17,700	2005
Rhizosolenia	*setigera*	381,500	2006-1/06-2/07/08/09

Appendix 2

See Table 5.

Table 5 Classification of heterotrophic microzooplankton into functional groups

Genus/group	Epitheton	Cell volume (μm^3)	Detected
Edible microzooplankton (EMZ)			
Smaller ciliates (CS)			
Myrionecta	*rubra*	4,510–27,361	2005/06-2/07/08/09
Mesodinium	*pulex*	4,188	2009
Lohmaniella	*oviformis*	4,510–6,478	2005/06-2/07/08/09
Diophrys	sp.	6,291	2006-2/07
Balanion	*comatum*	2,482	2005/06-2/07/09
Euplotes	sp.	5,994–14,762	2005/06-2/07/08/09
Strombidium	*emergens*	4,435	2009
Leegaardiella	*sol*	498	2006-2/09
Larger ciliates (CL)			
Scuticociliates		5,324–28,182	2005/06-2/07/09
Strobilidium	sp.	10,169–18,173	2005/06-2/07/08/09
Strobilidium	*conicum*	17,920	2005
Strobilidium	*neptunii*	36,192	2006-2/07
Strombidium	sp.	4,722–15,902	2005/06-2/07/09
Strombidium	*caudatum*	22,179	2006-2
Strombidium	*styliferum*	19,123	2005
Strombidium	*capitatum*	23,090	2009
Rimostrombidium	sp.	50,771	2009
Strobilid	sp.	22,017	2009
Laboea	*strobila*	28,672	2009
Tontonia	*gracilima*	32519–69,703	2005/06-2/07/09
Heterotrophic dinoflagellates (DINO)			
Gymnodiniales		5,394	2009
Gymnodinium	sp.	967–9,821	2007/08/09
Gyrodinium	sp.	9,977–17,284	2006-2/07/08/09
Diplopsalis	sp.	18,816	2009
Protoperidinium	sp.	9,521–40,045	2007/08
Protoperidinium	*bipes*	5,484–26,177	2007/09
Protoperidinium	*pellucidum*	40,045	2009
Protoperidinium	*brevipes*	29,503	2009
Protoperidinium	*ovatum*	126,292	2009
Peridinium	sp.	14,137	2009
Inedible microzooplankton (IMZ)			
Suctoria	sp.	18,500–19,299	$2005/06_2/07$
Acineta	sp.	19,033	2009
Tintinids		17,920–57,619	$2005/06_2/07/08/09$

Appendix 3

See Fig. 10

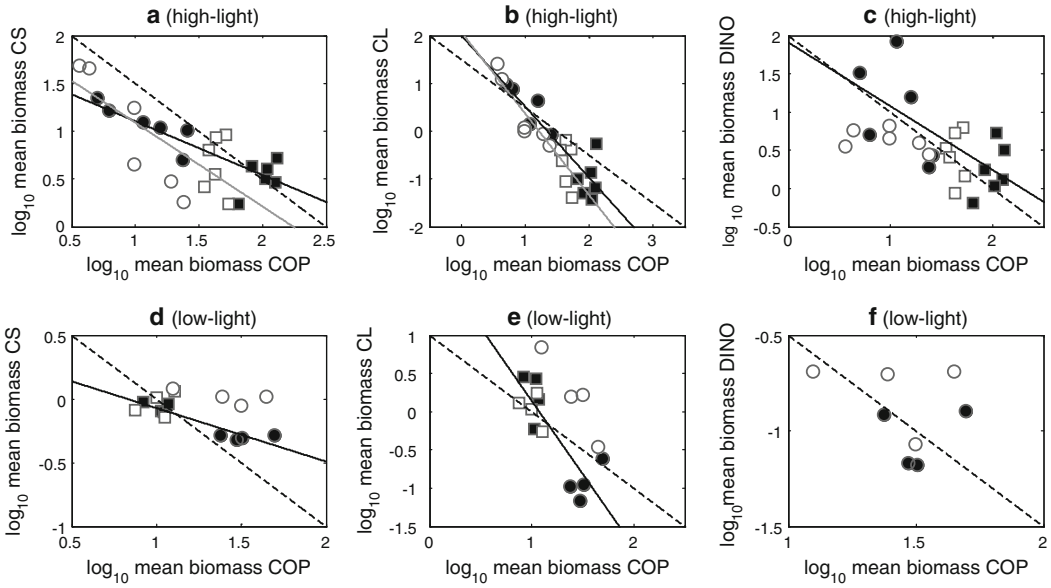

Fig. 10 Mean biomasses [μg C L^{-1}] of (**a**, **d**) smaller (CS) and (**b**, **e**) larger ciliates (CL) and (**c**, **f**) heterotrophic dinoflagellates (DINO) in relation to the mean biomass [μg C L^{-1}] of copepods (COP) for the high-light (**a**–**c**) and low-light experiments (**d**–**f**). *White* and *black squares* indicate data from the ambient ($\Delta T = 0$ °C, $\Delta T = 2$ °C)- and warm ($\Delta T = 4$ °C, $\Delta T = 6$ °C)-temperature treatments, respectively. Data points of the years 2005 and 2008 are marked by *squares* and of the years 2007 and 2009 by *circles*. *Black* ($\Delta T = 4$ °C, $\Delta T = 6$ °C) and *grey* ($\Delta T = 0$ °C, $\Delta T = 2$ °C) *lines* represent significant ($P < 0.05$) linear regression *lines*. Dashed lines represent 1:1 relationships

Appendix 4

See Fig. 11

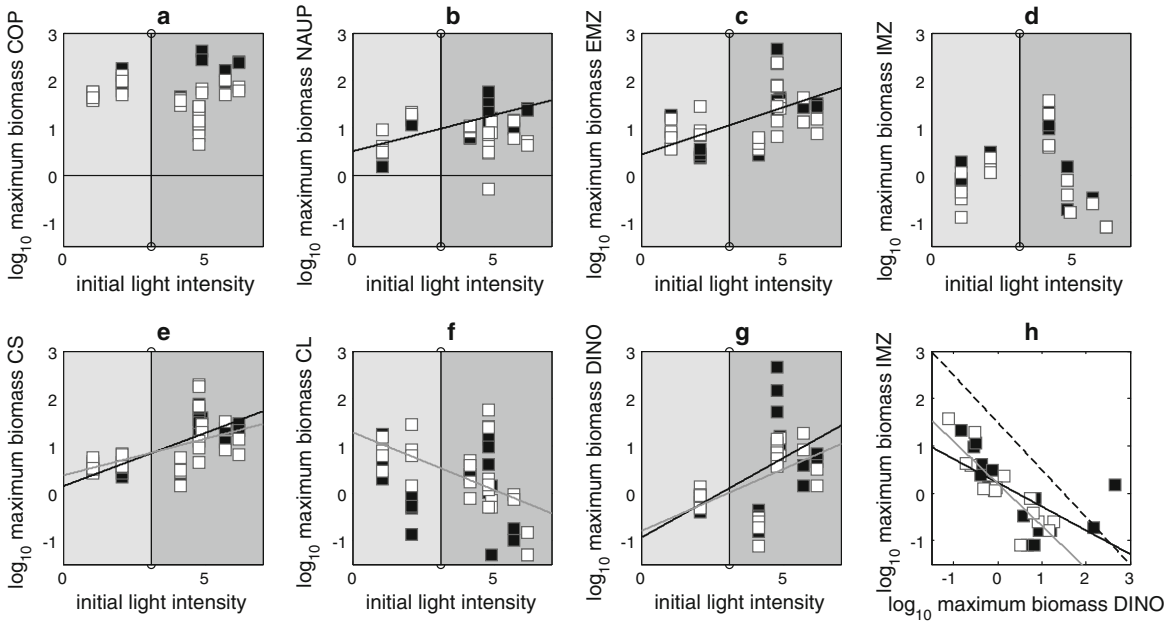

Fig. 11 Maximum biomasses [μg C L^{-1}] of **a** copepods (COP), **b** nauplii (NAUP), **c** edible microzooplankton (EMZ), **d** inedible microzooplankton (IMZ), **e** smaller (CS) and **f** larger ciliates (CL) and **g** heterotrophic dinoflagellates (DINO) in relation to the initial light intensity [Watt m^{-2} d^{-1}] of the experiments. **h** The maximum biomass of inedible microzooplankton (IMZ) in relation to the maximum biomass of DINO. *White* and *black* squares indicate data from the ambient ($\Delta T = 0$ °C, $\Delta T = 2$ °C)- and warm ($\Delta T = 4$ °C, $\Delta T = 6$ °C)-temperature treatments, respectively. The low-light and high-light experiments are marked *light* and *dark grey*. *Black* ($\Delta T = 6$ °C) and *grey* ($\Delta T = 0$ °C) *lines* represented significant ($P < 0.05$) linear regression *lines*. *Dashed lines* represent 1:1 relationships

References

Aberle N, Lengfellner K, Sommer U (2007) Spring bloom succession, grazing impact and herbivore selectivity of ciliate communities in response to winter warming. Oecologia 150:668–681. doi:10.1007/s00442-006-0540-y

BACC Author Team (2008) Assessment of climate change for the Baltic Sea Basin. Springer-Verlag, Berlin

Barber RT, Hiscock MR (2006) A rising tide lifts all phytoplankton: growth response of other phytoplankton taxa in diatom-dominated blooms. Global Biogeochem Cycles 20:GB4S03. doi:10.1029/2006GB002726

Barton BT, Beckerman AP, Schmitz OJ (2009) Climate warming strengthens indirect interactions in an old-field food web. Ecology 90:2346–2351. doi:10.1890/08-2254.1

Baumert HZ, Petzoldt T (2008) The role of temperature, cellular quota and nutrient concentrations for photosynthesis, growth and light-dark acclimation in phytoplankton. Limnologica 38:313–326. doi:10.1016/j.limno.2008.06.002

Beveridge OS, Petchey OL, Humphries S (2010a) Direct and indirect effects of temperature on the population dynamics and ecosystem functioning of aquatic microbial ecosystems. J Animal Ecol 79:1324–1331. doi:10.1111/j.1365-2656.2010.01741.x

Beveridge OS, Humphries S, Petchey OL (2010b) The interacting effects of temperature and food chain length on trophic abundance and ecosystem function. J Animal Ecol 79:693–700. doi:10.1111/j.1365-2656.2010.01662.x

Boyce DG, Lewis MR, Worm B (2010) Global phytoplankton decline over past century. Nature 466:591–596. doi:10.1038/nature09268

Bramm ME, Lassen MK, Liboriussen L, Richardson K, Ventura M, Jeppesen E (2009) The role of light for fish–zooplankton–phytoplankton interactions during winter in shallow lakes—a climate change perspective. Freshwater Biol 54:1093–1109. doi:10.1111/j.1365-2427.2008.02156.x

Brock TD (1981) Calculating solar radiation for ecological studies. Ecological modelling, 14rd edn, pp 1–19

Calbet A (2008) The trophic roles of microzooplankton in marine systems. ICES J Mar Sci 65:325–331. doi:10.1093/icesjms/fsn013

Calbet A, Saiz E (2005) The ciliate-copepod link in marine ecosystems. Aquat Microb Ecol 38:157–167. doi:10.3354/ame038157

Daufresne M, Lengfellner K, Sommer U (2009) Global warming benefits the small in aquatic ecosystems. Proc Nat Acad Sci USA 106:12788–12793. doi:10.1073/pnas.0902080106

Duffy JE, Stachowicz JJ (2006) Why biodiversity is important to oceanography: potential roles of genetic, species, and trophic diversity in pelagic ecosystem processes. Mar Ecol Prog Ser 311:179–189. doi:10.3354/meps311179

Finkel ZV, Beardall J, Flynn KJ, Quigg A, Rees TAV, Raven JA (2010) Phytoplankton in a changing world: cell size and elemental stoichiometry. J Plankton Res 32:119–137. doi:10.1093/plankt/fbp098

Gaedke U, Ruhenstroth-Bauer M, Wiegand I, Tirok K, Aberle N, Breithaupt P, Lengfellner K, Wohlers J, Sommer U (2010) Biotic interactions may overrule direct climate effects on spring phytoplankton dynamics. Glob Change Biol 16:1122–1136. doi:10.1111/j.1365-2486.2009.02009.x

Gargas E (1975) A manual for phytoplankton primary production studies in the Baltic. BMB Publishing, Horsholm, Danemark, Water Quality Institute 2

Guinder VA, Popovich CA, Molinero JC, Perillo GME (2010) Long-term changes in phytoplankton phenology and community structure in the Bahía Blanca Estuary, Argentina. Mar Biol 157:2703–2716. doi:10.1007/s00227-010-1530-5

Hansen B, Bjørnsen PK, Hansen PJ (1994) The size ratio between planktonic predators and their prey. Limnol Oceanogr 39:395–403

Hansen PJ, Bjørnsen PK, Hansen BW (1997) Zooplankton grazing and growth: scaling within the 2–2,000-µm body size range. Limnol Oceanogr 42:687–704

Henriksen P (2009) Long-term changes in the phytoplankton in the Kattegat, the Belt Sea, the Sound and the western Baltic Sea. J Sea Res 61:114–123. doi:10.1016/j.seares.2008.10.003

Hillebrand H, Dürselen CD, Kischtel K, Pollingher U (1999) Biovolume calculations for pelagic and benthic microalgae. J Phycol 35:403–424. doi:10.1046/j.1529-8817.1999.3520403.x

Hoekman D (2010) Turning up the heat: temperature influences the relative importance of top–down and bottom–up effects. Ecology 91:2819–2825. doi:10.1890/10-0260.1

Horn H, Horn W (2008) Bottom–up or top–down—how is the autotrophic picoplankton mainly controlled? Results of long-term investigations from two drinking water reservoirs of different trophic state. Limnologica 38:302–312. doi:10.1016/j.limno.2008.05.007

Ingrid G, Andersen T, Vadstein O (1996) Pelagic food webs and eutrophication of coastal waters: impact of grazers on algal communities. Mar Pollut Bull 33:22–35. doi:10.1016/S0025-326X(96)00134-8

IPCC (2007) Climate Change 2007: The Physical Science Basis. Contribution of Working Group I to the Fourth Assessment Report of the Intergovernmental Panel on Climate Change [Solomon S, Qin D, Manning M, Chen Z, Marquis M, Averyt KB, Tignor M, Miller HL (eds.)]. Cambridge University Press, Cambridge, United Kingdom and New York, NY, USA, p 996

Irigoien X, Flynn KJ, Harris RP (2005) Phytoplankton blooms: a 'loophole' in microzooplankton grazing impact? J Plankton Res 27:313–321. doi:10.1093/plankt/fbi011

Isla JA, Lengfellner K, Sommer U (2008) Physiological response of the copepod *Pseudocalanus* sp. in the Baltic Sea at different thermal scenarios. Glob Change Biol 14:895–906. doi:10.1111/j.1365-2486.2008.01531.x

Jakobsen HH, Halvorsen E, Hansen BW, Visser AW (2005) Effects of prey motility and concentration on feeding in *Acartia tonsa* and *Temora longicornis*: the importance of feeding modes. J Plankton Res 27:775–785. doi:10.1093/plankt/fbi051

Johansson M, Gorokhova E, Larsson U (2004) Annual variability in ciliate community structure, potential prey and predators in the open northern Baltic Sea proper. J Plankton Res 26:67–80. doi:10.1093/plankt/fbg115

Juliano SA (2001) Nonlinear curve fitting: predation and functional response curves. In: Scheiner SM, Gurevitch J (eds) Design and analysis of ecological experiments. Oxford University Press, Oxford, pp 178–196

Kleppel GS (1993) On the diets of calanoid copepods. Mar Ecol Prog Ser 99:183–195

Lehmann A, Getzlaff K, Harlass J (2011) Detailed assessment of climate variability in the Baltic Sea area for the period 1958–2009. Climate Research 46:185–196. doi:10.3354/cr00876

Lewandowska A (2011) Effects of warming on the phytoplankton succession and trophic interactions. Dissertation, Kiel University, Germany

Lewandowska A, Sommer U (2010) Climate change and the spring bloom: a mesocosm study on the influence of light and temperature on phytoplankton and mesozooplankton. Mar Ecol Prog Ser 405:101–111. doi:10.3354/meps08520

Litchman E, Pinto PT, Klausmeier CA, Thomas MK, Yoshiyama K (2010) Linking traits to species diversity and community structure in phytoplankton. Hydrobiologia 653:15–28. doi:10.1007/s10750-010-0341-5

Löder MGJ, Kraberg AC, Aberle N, Peters S, Wiltshire KH (2011a) Dinoflagellates and ciliates at Helgoland Roads, North Sea. Helgoland Marine Research. doi. doi:10.1007/s10152-010-0242-z

Löder MGJ, Meunier C, Wiltshire KH, Boersma M, Aberle N (2011b) The role of ciliates, heterotrophic dinoflagellates and copepods in structuring spring plankton communities at Helgoland Roads, North Sea. Mar Biol 158:1551–1580. doi:10.1007/s00227-011-1670-2

Lundsgaard C, Olesen M, Reigstad M, Olli K (1999) Sources of settling material: aggregation and zooplankton mediated fluxes in the Gulf of Riga. J Mar Syst 23:197–210

McCauley E, Briand F (1979) Zooplankton grazing and phytoplankton species richness: field tests of the predation hypothesis. Limnol Oceanogr 24:243–252

Menden-Deuer S, Lessard EJ (2000) Carbon to volume relationships for dinoflagellates, diatoms, and other protist plankton. Limnol Oceanogr 45:569–579

Montagnes DJS (1996) Growth responses of planktonic ciliates in the genera Strobilidium and Strombidium. Marine Ecology-Progress Series 130:241–254

Neumann T (2010) Climate-change effects on the Baltic Sea ecosystem: a model study. J Mar Syst 81:213–224. doi:10.1016/j.jmarsys.2009.12.001

O'Connor MI (2009) Warming strengthens an herbivore—plant interaction. Ecology 90:388–398. doi:10.1890/08-0034.1

O'Connor MI, Piehler MF, Leech DM, Anton A, Bruno JF (2009) Warming and resource availability shift food web structure and metabolism. PLoS Biol 7:e1000178. doi:10.1371/journal.pbio.1000178

Piontek J, Händel N, Langer G, Wohlers J, Riebesell U, Engel A (2009) Effects of rising temperature on the formation and microbial degradation of marine diatom aggregates. Aquat Microb Ecol 54:305–318. doi:10.3354/ame01273

Ptacnik R, Sommer U, Hansen T, Martens V (2004) Effects of microzooplankton and mixotrophy in an experimental planktonic food web. Limnol Oceanogr 49:1435–1445

Putt M, Stoecker DK (1989) An experimentally determined carbon: volume ratio for marine "Oligotrichous" ciliates from estuarine and coastal waters. Limnol Oceanogr 34:1097–1103

Reynolds CS (2006) The ecology of phytoplankton. Cambridge University Press, Cambridge

Richardson AJ (2008) In hot water: zooplankton and climate change. Journal of Marine Science 65:279–295. doi:10.1093/icesjms/fsn028

Richardson AJ, Schoeman DS (2004) Climate impact on plankton ecosystems in the Northeast Atlantic. Science 305:1609–1612. doi:10.1126/science.1100958

Rose JM, Caron DA (2007) Does low temperature constrain the growth rates of heterotrophic protists? Evidence and implications for algal blooms in cold waters. Limnol Oceanogr 52:886–895

Ryther JH, Sanders JG (1980) Experimental evidence of zooplankton control of the species composition and size distribution of marine phytoplankton. Mar Ecol Prog Ser 3:279–283. doi:10.3354/meps003279

Saiz E, Calbet A (2011) Copepod feeding in the ocean: scaling patterns, composition of their diet and the bias of estimates due to microzooplankton grazing during incubations. Hydrobiologia 666:181–196. doi:10.1007/s10750-010-0421-6

Sherr EB, Sherr BF (2007) Heterotrophic dinoflagellates: a significant component of microzooplankton biomass and major grazers of diatoms in the sea. Marine Ecology-Progress Series 352:187–197. doi:10.3354/meps07161

Sherr EB, Sherr BF (2009) Capacity of herbivorous protists to control initiation and development of mass phytoplankton blooms. Aquat Microb Ecol 57:253–262. doi:10.3354/ame01358

Sinistro R (2010) Top–down and bottom–up regulation of planktonic communities in a warm temperate wetland. J Plankton Res 32:209–220. doi:10.1093/plankt/fbp114

Smith JRWO, Lancelot C (2004) Bottom–up versus top–down control in phytoplankton of the Southern Ocean. Antarct Sci 16:531–539. doi:10.1017/S0954102004002305

Sommer U (2005) Biologische Meereskunde, 2nd edn. Springer, Berlin

Sommer U, Lengfellner K (2008) Climate change and the timing, magnitude, and composition of the phytoplankton spring bloom. Glob Change Biol 14:1199–1208. doi:10.1111/j.1365-2486.2008.01571.x

Sommer U, Lewandowska A (2011) Climate change and the phytoplankton spring bloom: warming and overwintering zooplankton have similar effects on phytoplankton. Glob Change Biol 17:154–162. doi:10.1111/j.1365-2486.2010.02182.x

Sommer U, Sommer F (2006) Cladocerans versus copepods: the cause of contrasting top-down controls on freshwater and marine phytoplankton. Oecologia 147:183–194. doi:10.1007/s00442-005-0320-0

Sommer U, Stibor H (2002) Copepoda–Cladocera–Tunicata: the role of three major mesozooplankton groups in pelagic food webs. Ecol Res 17:161–174. doi:10.1046/j.1440-1703.2002.00476.x

Sommer F, Saage A, Santer B, Hansen T, Sommer U (2005a) Linking foraging strategies of marine calanoid copepods to patterns of nitrogen stable isotope signatures in a mesocosm study. Marine Ecology-Progress Series 286:99–106. doi:10.3354/meps286099

Sommer U, Hansen T, Blum O, Holzner N, Vadstein O, Stibor H (2005b) Copepod and microzooplankton grazing in mesocosms fertilised with different Si:N ratios: no overlap between food spectra and Si:N influence on zooplankton trophic level. Oecologia 142:274–283. doi:10.1007/s00442-004-1708-y

Sommer U, Aberle N, Engel A, Hansen T, Lengfellner K, Sandow M, Wohlers J, Zöllner E, Riebesell U (2007) An indoor mesocosm system to study the effect of climate change on the late winter and spring succession of Baltic Sea phyto- an zooplankton. Oecologia 150:655–667. doi:10.1007/s00442-006-0539-4

Stibor H, Vadstein O, Diehl S, Gelzleichter A, Hansen T, Hantzsche F, Katechakis A, Lippert B, Løseth K, Peters C, Roederer W, Sandow M, Sundt-Hansen L, Olsen Y (2004) Copepods act as a switch between alternative trophic cascades in marine pelagic food webs. Ecol Lett 7:321–328. doi:10.1111/j.1461-0248.2004.00580.x

Tadonleke RD, Sime-Ngado T (2000) Rates of growth and microbial grazing mortality of phytoplankton in a recent artificial lake. Aquat Microb Ecol 22:301–313. doi:10.3354/ame022301

Thackeray SJ, Jones ID, Maberly SC (2008) Long-term change in the phenology of spring phytoplankton: species-specific responses to nutrient enrichment and climatic change. J Ecol 96:523–535. doi:10.1111/j.1365-2745.2008.01355.x

Tillmann U (2004) Interactions between planktonic microalgae and protozoan grazers. Journal of Eukayotic Microbiology 51:156–168

Tilzer MM, Elbrächter M, Gieskes WW, Beese B (1986) Light-temperature interactions in the control of photosynthesis in Antarctic phytoplankton. Polar Biol 5:105–111. doi:10.1007/BF00443382

Vadstein O, Stibor H, Lippert B, Løseth K, Roederer W, Sundt-Hansen L, Olsen Y (2004) Moderate increase in the biomass of omnivorous copepods may ease grazing control of planktonic algae. Mar Ecol Prog Ser 270:199–207. doi:10.3354/meps270199

Vincent D, Hartmann HJ (2001) Contribution of ciliated microprotozoans and dinoflagellates to the diet of three copepod species in the Bay of Biscay. Hydrobiologia 443:193–204. doi:10.1023/A:1017502813154

Wasmund N, Göbel J, Von Bodungen B (2008) 100-years-changes in the phytoplankton community of Kiel Bight (Baltic Sea). J Mar Syst 73:300–322. doi:10.1016/j.jmarsys.2006.09.009

Wiklund AKE, Dahlgren K, Sundelin B, Andersson A (2009) Effects of warming and shifts of pelagic food web structure on benthic productivity in a coastal marine system. Mar Ecol Prog Ser 396:13–25. doi:10.3354/meps08290

Wiltshire KH, Malzahn AM, Wirtz K, Greve W, Janisch S, Mangelsdorf P, Manly BFJ, Boersma M (2008) Resilience of North Sea phytoplankton spring bloom dynamics: an analysis of long-term data at Helgoland Roads. Limnol Oceanogr 53:1294–1302. doi:10.4319/lo.2008.53.4.1294

Wiltshire KH, Kraberg A, Bartsch I, Boersma M, Franke HD, Freund J, Gebühr C, Gerdts G, Stockmann K, Wichels A (2010) Helgoland Roads, North Sea: 45 years of change. Estuaries Coasts 33:295–310. doi:10.1007/s12237-009-9228-y

Winder M, Reuter JE, Schladow SG (2009) Lake warming favours small-sized planktonic diatom species. Proceedings of the Royal Society B—Biological Sciences 276:427–435. doi:10.1098/rspb.2008.1200

Wohlers J, Engel A, Zöllner E, Breithaupt P, Jürgens K, Hoppe HG, Sommer U, Riebesell U (2009) Changes in biogenic carbon flow in response to sea surface warming. Proc Nat Acad Sci USA 106:7067–7072. doi:10.1073/pnas.0812743106

Yvon-Durocher G, Montoya JM, Trimmer M, Woodward G (2011) Warming alters the size spectrum and shifts the distribution of biomass in freshwater ecosystems. Glob Change Biol 17:1681–1694. doi:10.1111/j.1365-2486.2010.02321.x

Zöllner E, Santer B, Boersma M, Hoppe HG, Jürgens K (2003) Cascading predation effects of Daphnia and copepods on microbial food web components. Freshw Biol 48:2174–2193. doi:10.1046/j.1365-2426.2003.01158.x

Zöllner E, Hoppe HG, Sommer U, Jürgens K (2009) Effect of zooplankton-mediated trophic cascades on marine microbial food web components (bacteria, nanoflagellates, ciliates). Limnol Oceanogr 54:262–275. doi:10.4319/lo.2009.54.1.0262